2 *Carbon dioxide assimilation and respiration*

Chapter 2 quote to come

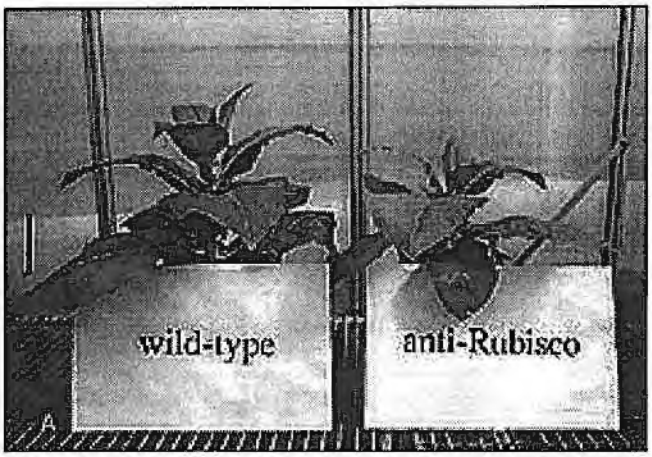

Rubisco (ribulose-1,5-bisphosphate carboxylase/oxygenase) is the most abundant single protein on earth and is pivotal for CO_2 assimilation by all plants. In higher plants, the holoenzyme consists of eight large subunits, each with a molecular mass of 50–55 kD (identified in (b) below), and eight small subunits of molecular mass 12–18 kD (not shown). Large subunits are encoded by a single gene in the chloroplast genome while a family of nuclear genes encode the small subunits.

Any loss of catalytic effectivess or reduction in amount translates to slower photorynthesis and reduced growth. Tobacco plants (a) transformed with an antisense construct against Rubisco (anti-Rubisco) grow more slowly than wild types due to a 60% reduction in photosynthetic rate. Immunodetection of the large subunit polypeptide of Rubisco with an anti-Rubisco antiserum (b) shows that the anti-Rubisco transgenic plants contain less than 50% of the Rubisco detected in wild-type tobacco plants. (Vertical bar in (a) = 10 cm)
(Photo courtesy Susanne von Caemmerer; original immunoblot courtesy Martha Ludwig)

Chapter outline

Introduction

Life on earth is carbon based and is sustained by photosynthetic use of energy from sunlight to fix atmospheric CO_2. With evolution of life, primitive photoautotrophs gave rise to vascular plants which in turn adapted to changing aquatic and terrestrial environments via distinctive modes of photosynthesis.

Features of C_3, C_4 CAM and SAM photosynthesis (Section 2.1) highlight the central significance of Rubisco and outline metabolic extensions to that basic process that have enabled adaptation to arid regions (CAM) and aquatic environments (SAM), or have led to spectacular gains in photosynthetic capacity of C_4 plants (C_4 subgroups in Section 2.2).

Paradoxically, oxygenic photosynthesis in C_3 plants is actually inhibited by oxygen! This outcome has major implications for global productivity and holds special relevance for comparative performance of C_3 and C_4 plants. Recognition of such O_2-dependent photorespiratory loss of carbon from C_3 plants but not from C_4 plants represented a major paradigm shift in plant science and is recounted in Section 2.3.

Finally, a significant fraction of the carbon gained via photosynthesis becomes a respiratory substrate for generation of energy to sustain vital processes, as well as providing carbon skeletons for a multitude of synthetic events (Section 2.4).

2.1 Modes of photosynthesis

Millions of years of evolution have produced significant biochemical variants for fixation of atmospheric CO_2 into carbohydrate, namely (1) C_3 (three-carbon fixation product), (2) C_4 (four-carbon fixation product), (3) CAM (crassulacean acid metabolism) and (4) SAM (submerged aquatic macrophytes).

Despite much diversity in life form and biochemical process, all of these pathways focus upon a single enzyme which is by far the most abundant protein on earth, namely ribulose-1,5-bisphosphate carboxylase/oxygenase, or Rubisco (Figure 2.1a). Localised in the stroma of chloroplasts, this enzyme enables the primary catalytic step in photosynthetic carbon reduction (or PCR cycle) in all green plants and algae (Bassham and Calvin 1957). Although Rubisco has been highly conserved throughout evolutionary history, this enzyme is surprisingly inefficient with a slow turnover of active sites and a rather feeble discrimination between alternative substrates (CO_2 and O_2), a combination that severely restricts photosynthetic performance of C_3 plants under ambient conditions of 20% O_2 and 0.035% CO_2. Accordingly, and in response to CO_2 limitation, C_4, CAM and SAM variants have evolved with metabolic concentrating devices which enhance Rubisco performance.

2.1.1 Photosynthetic carbon reduction

The biochemical pathway of CO_2 fixation was discovered by feeding radioactively labelled CO_2 in the light to algae and then extracting the cells and examining which compounds accumulated radioactivity. Figure 2.1 (b) shows a typical labelling 'pattern' for a C_3 plant. Here, a short burst of labelled CO_2 was given to the plants, then the label was 'chased' through the photosynthetic pathway by flushing with unlabelled air. Atmospheric CO_2 is initially incorporated into a five-carbon sugar phosphate (ribulose-1,5-bisphosphate or RuBP) to produce two molecules of the phosphorylated three-carbon compound 3-phosphoglycerate, often referred to as the acidic form 3-phosphoglyceric acid (3-PGA). Hence, plants which use Rubisco as their primary enzyme of CO_2 fixation from the air are called C_3 plants. Consequently, in C_3 plants, 3-PGA is the first labelled sugar phosphate detected after a pulse of $^{14}CO_2$ has been supplied (Figure 2.1b). In the PCR cycle, 3-PGA is phosphorylated by the ATP produced from thylakoid electron transport (Section 1.3) and then reduced by NADPH to produce triose phosphate. Triose phosphate is the first stable product from Rubisco activity.

Newly synthesised triose phosphate faces three options. It can be (1) exported to the cytosol for sucrose synthesis and subsequent translocation to the rest of the plant, (2) recycled within the chloroplast to produce more RuBP or (3) diverted to produce starch (see Figure 2.1 a, and starch grain in Figure 2.1.9). This is shown by the time-course of the appearance of radioactivity in starch and sucrose after it has passed through 3-PGA (Figure 2.1b). The energy requirements of the PCR cycle are three ATP and two NADPH per CO_2 fixed, in the absence of any other energy-consuming processes.

2.1.2 RuBP regeneration

Ribulose bisphosphate (RuBP) is consumed in the carboxylating step of carbon fixation. If such fixation is to continue,

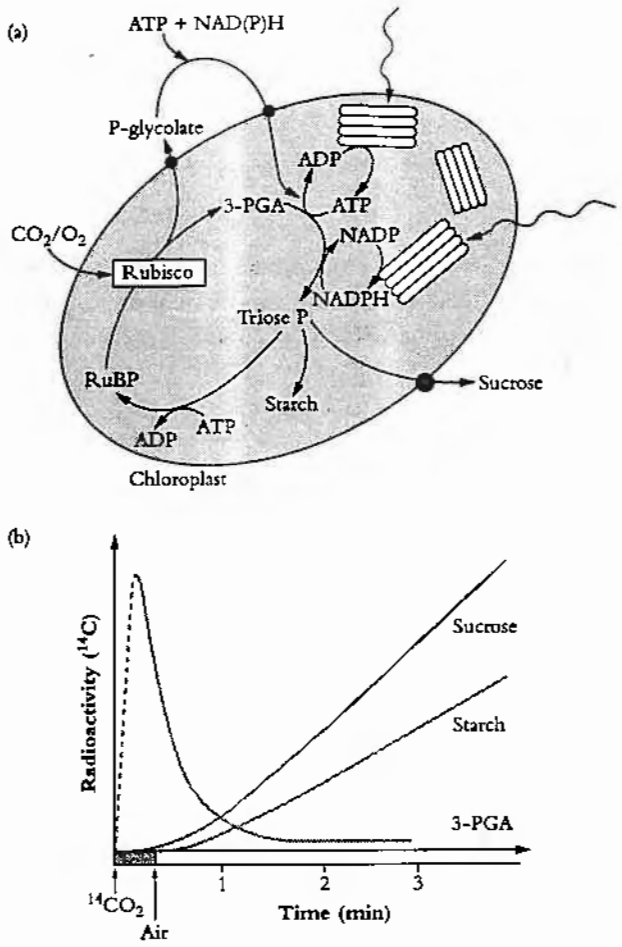

Figure 2.1 Photosynthetic carbon reduction (PCR cycle) utilises ATP and NADPH produced by thylakoid electron transport to drive CO_2 fixation by Rubisco (a). CO_2 is incorporated into a five-carbon sugar phosphate to produce two three-carbon sugar phosphates which can either be exported from the chloroplast for sucrose synthesis, be recycled to make more five-carbon acceptors or be used to make starch. The appearance of radioactive carbon in three-carbon sugar phosphates and then in starch and sucrose following photosynthesis in $^{14}CO_2$ was evidence for the pathway of photosynthesis (b) (Original drawing courtesy Bob Furbank)

RuBP must be regenerated, and in this case via the PCR cycle. The PCR cycle operates within the stroma of chloroplasts, and consists of a sequence of 11 steps where a three-carbon compound (3-phosphoglycerate) is phosphorylated, reduced to glyceraldehyde 3-phosphate and isomerised to dihydroxyacetone phosphate. Condensation of this three-carbon compound with glyceraldehyde 3-phosphate yields a six-carbon compound (fructose bisphosphate). Following a series of carbon shunts, involving four-, five- and seven-carbon compounds, RuBP is regenerated.

Important features of the PCR cycle include: (1) for every step of the cycle to occur once, three carboxylations must occur via ribulose bisphosphate carboxylase thus generating six moles of phosphoglycerate (18 carbons); (2) for one turn of the cycle, three molecules of RuBP participate (15 carbons) and thus a net gain of three carbons has occurred for the plant; (3) in regenerating three molecules of RuBP, nine ATPs and six NADPHs are consumed.

2.1.3 Sucrose and starch synthesis

Most of the triose phosphate synthesised in chloroplasts is converted to either sucrose or starch. Starch accumulates in chloroplasts, but sucrose is synthesised in the surrounding cytosol, starting with the export of dihydroxyacetone phosphate and glyceraldehyde phosphate from the chloroplast. A condensation reaction, catalysed by aldolase, generates fructose-1,6-bisphosphate, and this is converted to fructose-6-phosphate after an hydrolysis reaction catalysed by fructose-1,6-phosphatase. Sucrose-6-phosphate synthase then generates sucrose-6-phosphate from the reaction of fructose-6-phosphate and UDP-glucose. The phosphate group is removed by the action of sucrose-6-phosphatase. This P_i is transported back into the chloroplast where it is available for ATP synthesis. For each molecule of triose phosphate exported from a chloroplast, one P_i is translocated inwards. This stoichiometric link operates via a P_i-triose phosphate antiport system (Figure 2.8).

Sucrose synthesised within the cytosol of photosynthesising cells is then available for general distribution and is commonly translocated to other carbon-demanding centres via the phloem (Section 5.1).

By contrast, starch synthesis occurs within chloroplasts. The first step is a condensation of glucose-1-phosphate with ATP. Starch synthase then transfers glucose residues from this molecule to the non-reducing end of a pre-existing molecule of starch. Starch consists of two types of glucose polymer, namely amylose and amylopectin. Amylose is a long, unbranched chain of D-glucose units connected via (α1–4) linkages. Amylopectin is a branched form, with (α1–6) linkages forming branches approximately every 24–30 glucose residues.

2.1.4 Properties of Rubisco

Photosynthetic carbon fixation in air is constrained by the kinetic properties of Rubisco (reviewed by Woodrow and Berry 1988; see also Section 2.2 and 2.3). Rubisco is a huge protein and despite selection pressure over evolutionary history remains an inefficient catalyst (Andrews and Lorimer 1987). Plants compensate by investing large amounts of nitrogen in Rubisco which then comprises more than 50% of leaf protein in C_3 plants. On a global scale, this investment equates to around 10 kg of nitrogen per person!

Something like 1000 million years of evolution has still not resulted in a 'better' Rubisco. Such a highly conserved catalytic protein is an outcome of thermodynamic and mechanistic difficulties inherent to this reaction. Rubisco first evolved when the earth's atmosphere was rich in CO_2, but virtually devoid of O_2. With the advent of oxygenic photosynthesis, increased partial pressure of atmospheric O_2 and

subsequent appearance of land plants, one key deficiency of this enzyme became apparent. Rubisco would not only catalyse fixation of CO_2 but would also permit incorporation of O_2 into RuBP to produce a molecule of 3-PGA and a molecule of 3-phosphoglycolate (Figure 2.1a). Indeed, CO_2 and O_2 actually compete directly for access to the same (CO_2) binding sites! So feeble is Rubisco's ability to distinguish between these two substrates that in air (20% O_2) approximately one molecule of O_2 is fixed for every three molecules of CO_2.

Fixation of O_2, and subsequent photorespiration (Section 2.3) is an energy-consuming process, due to competition between O_2 and CO_2 for RuBP, plus the energy cost of converting phosphoglycolate to a form which can be recycled in the PCR cycle (Section 2.3). This energy cost is increased at higher temperatures because O_2 competes more effectively with CO_2 at the active site of Rubisco (Lorimer and Andrews 1981). Such sensitivity to temperature × O_2 explains why CO_2 enrichment, which reduces photorespiration, has a proportionally larger effect upon net carbon gain at higher temperatures than at lower temperatures (Section 2.2).

Notwithstanding a meagre catalytic effectiveness in present-day Rubisco, more efficient variants would still have had a selective advantage, and especially during those times in the earth's geological history when atmospheric CO_2 concentration was decreasing. Indeed there has been some improvement (Figure 2.2) such that the specificity towards CO_2 over O_2 has sharpened significantly. Recently evolved angiosperms show a relative specificity almost twice that of 'older' organisms such as photosynthetic bacteria.

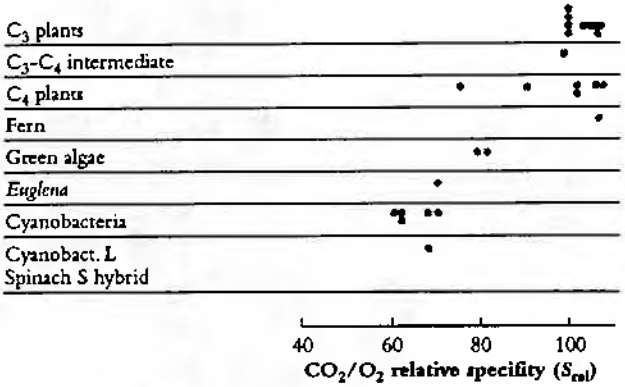

Figure 2.2 Mechanisms underlying CO_2 fixation by Rubisco have changed very little during evolution but Rubisco efficiency has improved. The enzyme in more 'highly evolved' species such as C_3 angiosperms is able to fix more CO_2 and less O_2 in air, reducing photorespiratory energy costs. A measure of this is the relative specificity of Rubisco for CO_2 (Srel), shown here for a range of photosynthetic organisms.
(Based on Andrews and Lorimer 1987)

Despite such improvement, Rubisco remains seemingly maladapted to its cardinal role in global carbon uptake, and in response to selection pressure for more efficient variants of CO_2 assimilation, vascular plants have evolved with photosynthetic mechanisms that alleviate an inefficient Rubisco. One key feature of such devices is a mechanism to increase CO_2 concentration at active sites within photosynthetic tissues. Some of these photosynthetic pathways are dealt with below.

FEATURE ESSAY 2.1 C_4 Photosynthesis

M.D. (Hal) Hatch

Discovering C_4 photosynthesis is an instructive story because it says a lot about progress in science, about serendipity, as well as mindsets and our natural resistance to accept results that conflict with the dogma of the day.

As a rule the major chemical transformations that occur in plants proceed by exactly the same series of steps in all species. For instance, take the process of respiration where sugars and starch are broken down to CO_2 and H_2O, yielding energy for living cells. It is almost certain that this proceeds by exactly the same 20 or so steps in species right across the Plant Kingdom. In fact, the same process also operates in yeast, mice and man.

During the 1950s Melvin Calvin and his colleagues at Berkeley resolved the mechanism of photosynthetic CO_2 assimilation in the alga Chlorella. Later, they showed that similar steps, with similar enzymes, occurred in a few higher plants. So, by the end of the 1950s it was reasonably assumed that this process, termed the calvin cycle or photosynthetic carbon reduction (PCR) cycle, accounted for CO_2 assimilation in all photosynthetic organisms.

In retrospect, a very observant reader of the plant biological literature of the early 1960s should have noticed that a small group of grass species, including plants like maize, had a set of very unusual but correlated properties, related in one way or another to the process of photosynthesis, that contrasted with the vast majority of other vascular plants. These included an unusual leaf anatomy, substantially higher rates of photosynthesis and growth, higher temperature and light optima for photosynthesis, a much higher water use efficiency, and a very low CO_2 compensation point. From this one might have reasonably concluded that these particular species could be using a different biochemical process for photosynthesis.

We now know that these unusual species fix CO_2 by the C_4 photosynthetic mechanism. However, the process was not discovered by following up these observations, and only later was the significance of these unusual correlated features fully appreciated.

During the early 1960s, my colleague Roger Slack and I were working on aspects of carbohydrate biochemistry

Figure 1 Dr M.D. (Hal) Hatch, FAA, FRS, primary discovere of C_4 photosynthesis

and sugar accumulation in sugar cane in the research laboratory of the Colonial Sugar Refining Company in Brisbane. Because of these particular interests, we were in regular contact with a laboratory in Hawaii that also worked on sugar cane. We learned from our Hawaiian colleagues Hart, Kortschak and Burr, that they had seen some unusual results when they allowed sugar cane leaves to fix radioactive carbon dioxide ($^{14}CO_2$), that is, doing the same experiment that Calvin and his colleagues had done earlier with Chlorella. With this procedure radioactivity should be initially incorporated into the first products formed when CO_2 is assimilated; in the case of the PCR cycle the radioactivity should appear in the three-carbon compound 3-phosphoglyceric acid (3-PGA) and then in sugar phosphates. However, when these Hawaiian workers first did this experiment as early as 1957 they saw only minor radiolabelling in 3-PGA after brief exposure to $^{14}CO_2$ and later they showed that most of the radioactivity was located in the four-carbon dicarboxylic acids, malate and aspartate.

We were really intrigued by this result and had often discussed possible interpretations and significance. So when the Hawaiian group published their results a few years later in 1965 we set about repeating and extending these observations to see if we could find out what it all meant.

Before coming to that work it is worth recounting one other interesting twist to the story. In the late 1960s, and several years after we had begun studying C_4 photosynthesis, we became aware of a report published some 10 years earlier in a somewhat obscure annual report of a Russian agricultural research institute. This report from a young Russian scientist, Yuri Karpilov, clearly showed that when maize leaves are exposed to radioactive CO_2 most of the radioactivity incorporated after 15 was not in 3-PGA acid but was in the same dicarboxylic acids, malate and aspartate, that the Hawaiians had found in labelled sugar cane leaves. In a publication about three years later, Karpilov and a more senior Russian scientist speculated that these results may have been due to faulty killing and extraction procedures. It seems doubtful that they appreciated the full significance of this earlier study.

Our initial experiments were designed to trace the exact fate of carbon assimilated by photosynthesis using $^{14}CO_2$. Sugar cane leaves were exposed to $^{14}CO_2$ for various periods under steady-state conditions for photosynthesis, then killed and extracted, and the radioactive products were separated by chromatography, identified and degraded to find out which carbons contained radioactivity. We confirmed the results of the Hawaiian group that most of the radioactivity incorporated after short periods in radioactive CO_2 was located in the four-carbon acids malate and aspartate. Substantial radioactive labelling of the PCR cycle intermediates occurred only after longer periods (minutes, rather than seconds).

Critical information was subsequently provided by our so-called 'pulse–chase' experiments where a leaf was dosed briefly with $^{14}CO_2$, and then returned to unlabelled air. The biochemical fate of previously fixed ^{14}C can be followed in sequential samples of tissue. These experiments clearly showed a rapid movement of radioactivity from the four-carbon acid malate into 3-PGA and then later to sugar phosphates and finally into sucrose and starch. There were additional critical results from these initial studies. (1) a chemically unstable dicarboxylic acid, oxaloacetic acid, was rapidly labelled as well as malate and aspartate and was almost certainly the true first product formed; (2) fixed CO_2 gave rise to the 4-C carboxyl of these four-carbon acids; and (3) this 4-C carboxyl carbon gave rise to the 1-C carboxyl of 3-PGA. Identification of oxaloacetic acid as an early labelled fixation product was an especially demanding task, and involved generation of a stable derivative that would remain intact during extraction and analysis of ^{14}C fixation products.

Spurred on by this success, we then surveyed a large number of species and found radioactive labelling patterns similar to sugar cane in a number of other grass species, including maize, as well as species from two other plant families. This was an exciting result for us at the time since it clearly showed that this mode of photosynthesis was reasonably widespread taxonomically. The next step in determining the exact nature of this process was to discover the enzymes involved. In species such as sugar cane and maize, there proved to be seven enzyme-catalysed reactions

involved in the steps unique to C_4 photosynthesis, and these included two steps catalysed by enzymes that had never been described before!

Soon after, we named this process the C_4 dicarboxylic acid pathway of photosynthesis — after the first product formed. This was later abbreviated to C_4 pathway or C_4 photosynthesis and the plants employing this process were termed C_4 plants.

By 1970 we had a reasonably good understanding of how C_4 photosynthesis worked in species like maize and sugar cane (see Section 2.1 for details), and suggested that the reactions unique to C_4 photosynthesis might function to concentrate CO_2 in the bundle sheath cells of C_4 leaves, acting essentially as a CO_2 pump. Later, we obtained direct experimental evidence that CO_2 was indeed concentrated about 10- to 20-fold in these cells in the light.

As I mentioned earlier, a major departure from Calvin-cycle photosynthesis was never expected. Imagine our surprise, therefore, when it was revealed during the early 1970s that there existed not one, but three different biochemical variants for C_4 photosynthesis. On this basis C_4 species were divided into three groups, and some connections between process and taxonomic background then emerged.

What advantages did all this offer plants over plants that fix CO_2 directly by the PCR cycle — that is, using CO_2 diffusing directly from air (and distinguished as C_3 plants by virtue of their initial three-carbon fixation product phosphoglycerate). As Section 2.1 explains, concentrating CO_2 in bundle sheath cells eliminates photorespiration. This, in turn, gives C_4 plants distinct advantages in terms of growth and survival, especially at higher temperatures and under strong light. This can be seen most graphically in the distribution of grass species in Australia. In Tasmania, as well as the cooler and wetter southern-most tips of the continent, C_4 species are in the minority. However, going north there is a rapid transition and for most of the continent most or all of the grass species are C_4 (discussed further in Chapter 14).

C_4 photosynthesis also offers a potential for growth rates almost twice those seen in C_3 plants, but this potential will only be seen at higher temperatures and higher light and this will not be evident in all C_4 species. With this kind of growth potential, it is not surprising that C_4 species also number among the world's worst weeds!

As a parting note I should add that about 100 million years ago C_3 plants were in their 'prime' with atmospheric CO_2 concentrations between five and ten times present-day levels. However, a new selection pressure then developed. Atmospheric CO_2 declined over the next 50–60 million years to something close to our twentieth century levels of about 350 μL–1. This decline almost certainly provided the driving force for evolution of C_4 photosynthesis. In other words, C_4 photosynthesis was originally 'discovered' by nature in the course of overcoming the adverse effects of lower atmospheric CO_2 concentration on C_3 plants. In effect, C_4 processes increase the CO_2 concentration in bundle sheath cells to somewhere near the atmospheric CO_2 concentration of 100 million years ago.

Further reading

Hatch, M.D. (1987), 'C4 photosynthesis: a unique blend of modified biochemistry, anatomy and ultrastructure', Biochimica Biophysica Acta, 895, 81–106.

Hatch, M.D. (1992). 'C4 photosynthesis: an unlikely process full of surprises', Plant Cell Physiology, 33, 333–342.

2.1.5 C_4 photosynthesis

Most vascular plants perform C_3 photosynthesis, including commercially significant cereals, broad-leafed herbaceous plants such as legumes and oil seeds as well as all tree species. However, some important modern groups that are phylogenetically derived from C_3 plants perform C_4 photosynthesis (see Hatch 1988 and feature essay 2.1). Plants in this group include maize, sugar cane, sorghum, a wide variety of tropical pasture grasses and most of the world's worst tropical weeds (such as crabgrass and nutgrass). C_4 plants are generally characterised by high rates of photosynthesis and growth, particularly in subtropical/tropical environments.

C_4 plants have a competitive advantage over C_3 plant at high temperature and under strong light because of a reduction in photorespiration plus an increase in absolute rates of CO_2 fixation at ambient CO_2. Such increase in photosynthetic efficiency results in faster carbon gain and commonly higher growth rates. The C_4 pathway (Figure 2.3) is 'a unique blend of modified biochemistry, anatomy and ultrastructure' (Hatch 1988). Initial and rapid fixation of CO_2 within mesophyll cells results in formation of a four-carbon compound which is then pumped to bundle sheath cells for decarboxylation and subsequent incorporation into the PCR cycle in that tissue. This neat division of labour hinges on specialised anatomy and has even resulted in evolution of distinct classes of chloroplasts in mesophyll compared with bundle sheath cells. Three variants of C_4 photosynthesis are known to have evolved from C_3 progenitors (Section 2.2) and in all cases with a recurring theme where the C_4 cycle of mesophyll cells is complemented by a PCR cycle in bundle sheath cells. In effect, a biochemical 'pump' concentrates CO_2 at Rubisco sites in bundle sheath cells thereby sustaining faster net rates of CO_2 incorporation and virtually eliminating photorespiration.

For this overall mechanism to have evolved, a complex combination of cell specialisation and differential gene expres-

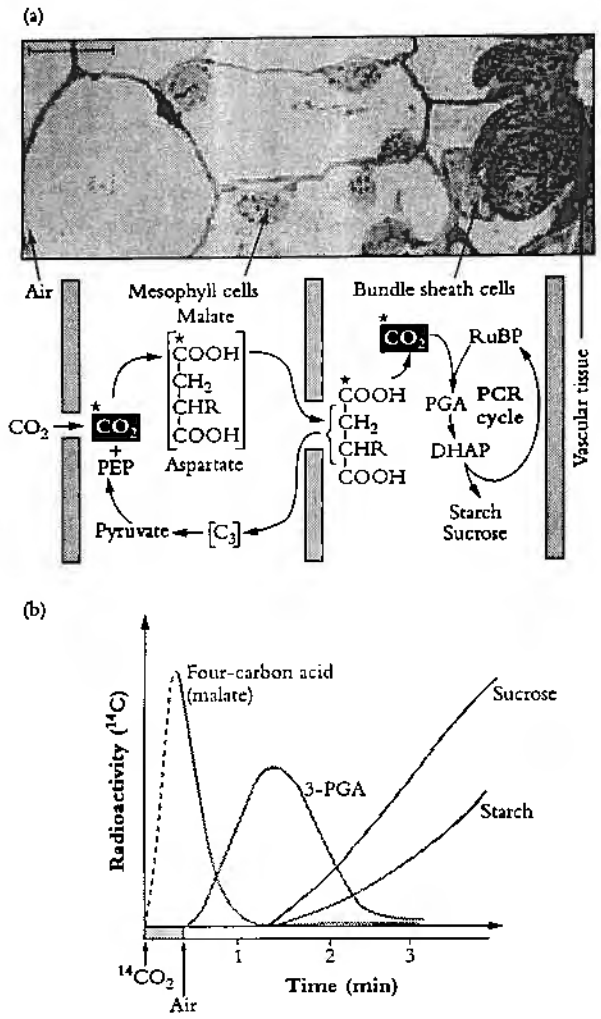

Figure 2.3 C_4 photosynthesis is an evolutionary development where specialised mesophyll cells initially fix CO_2 from the air into four-carbon acids which are transported to the site of the PCR cycle in the bundle sheath. The bundle sheath cells are relatively impermeable to CO_2, so that when the CO_2 is released here from the four-carbon acids, it builds up to high levels. The C_4 photosynthetic mechanism is a biochemical CO_2 pump. The pathway shown here is overlayed on a micrograph of a C_4 leaf, showing bundle sheath and mesophyll cells. Rubisco and the other PCR enzymes are in the bundle sheath cells while phosphoenolpyruvate (PEP) carboxylase is part of the CO_2 pump in the mesophyll cells. In C_4 plants, after radioactive labelling, ^{14}C appears first in a four-carbon acid, rather than in 3-PGA Horizontal bar = 10 μm. (Original drawings courtesy M.D. Hatch)

sion was necessary. Figure 2.3 shows a low-magnification electron micrograph of a C_4 leaf related to a generalised scheme for the C_4 pathway.

By analogy with Calvin's biochemical definition of the C_3 pathway at Berkeley in the 1950s, the C_4 pathway was also delineated with radioactively labelled CO_2 (see Feature essay 2.1). Significantly, and unlike C_3 plants, 3-PGA is not the first compound to be labelled after a ^{14}C pulse (Figure 2.3b). Specialised mesophyll cells carry out the initial steps of CO_2 fixation utilising the enzyme phosphoenolpyruvate (PEP) carboxylase. The product of CO_2 fixation, oxaloacetate, is a four-carbon organic acid, hence the designation 'C_4' photosynthesis (or colloquially, C_4 plant). A form of this C_4 acid, either malate or aspartate depending on the C_4 variant, migrates to the bundle sheath cells which contain Rubisco and the PCR cycle. In the bundle sheath cells, CO_2 is removed from the 4-carbon acid by a specific decarboxylase and a C_3 product returns to the mesophyll to be recycled to PEP for the carboxylation reaction. Thus, label appears in the 4-carbon acid first, after ^{14}C feeding and then in 3-PGA and, finally, sucrose and starch (Figure 2.1 b).

A physical barrier to CO_2 diffusion exists in the cell walls of the bundle sheath compartment (suberised lamellae), preventing CO_2 diffusion back to the mesophyll and allowing CO_2 build up to levels at least 10 times those of ambient air. Rubisco is thus exposed to a saturating concentration of CO_2 which both enhances carboxylation due to increased substrate supply, and forestalls oxygenation of RuBP (hence photorespiration) by outcompeting O_2 for CO_2-binding sites on Rubisco (Figure 2.4).

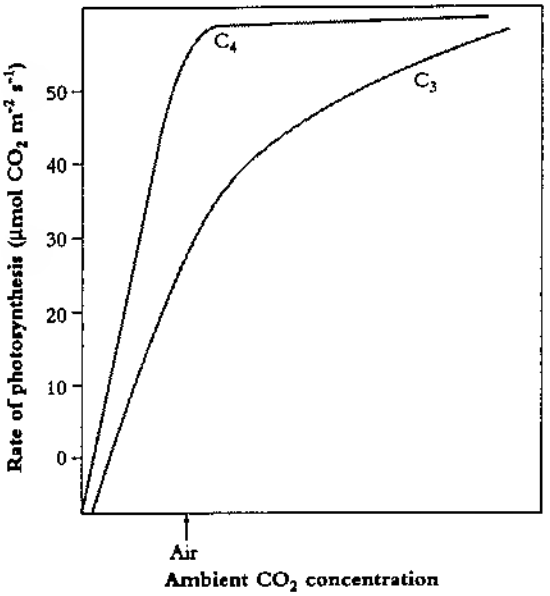

Figure 2.4 CO_2 photosynthesis response curves show that C_4 plants have a higher affinity for CO_2. At common ambient levels of CO_2, photosynthesis in a C_4 leaf is already almost fully expressed, whereas a C_3 plant is operating at only one-half to two-thirds maximum rate. This contrast is due to the CO_2-concentrating function of C_4 photosynthesis. More sophisticated measurement of leaf assimilation as a function of intercellular CO_2 (Figures 1–3 in Case study 1.1) can be used to reveal component processes (Original drawings courtesy M.D. Hatch)

In leaves of C_3 plants, the PCR cycle operates in all mesophyll chloroplasts, but in C_4 plants the PCR cycle is restricted to bundle sheath cells (Figure 2.3). Rubisco is pivotal in this cycle, and can be used as a marker for sites of photosynthetic carbon reduction. Rubisco can be visualised by localising this photosynthetic enzyme with antibodies via indirect immunofluorescent labelling (Figure 2.5a, b). In this pioneering method (Hattersley *et al.* 1977) 'primary' rabbit anti-Rubisco serum (from rabbits injected with purified Rubisco) is first applied to fixed transverse sections of leaves. Rabbit antibodies to Rubisco bind to the enzyme *in situ*. Then 'secondary' sheep anti-rabbit immunoglobulin tagged with a

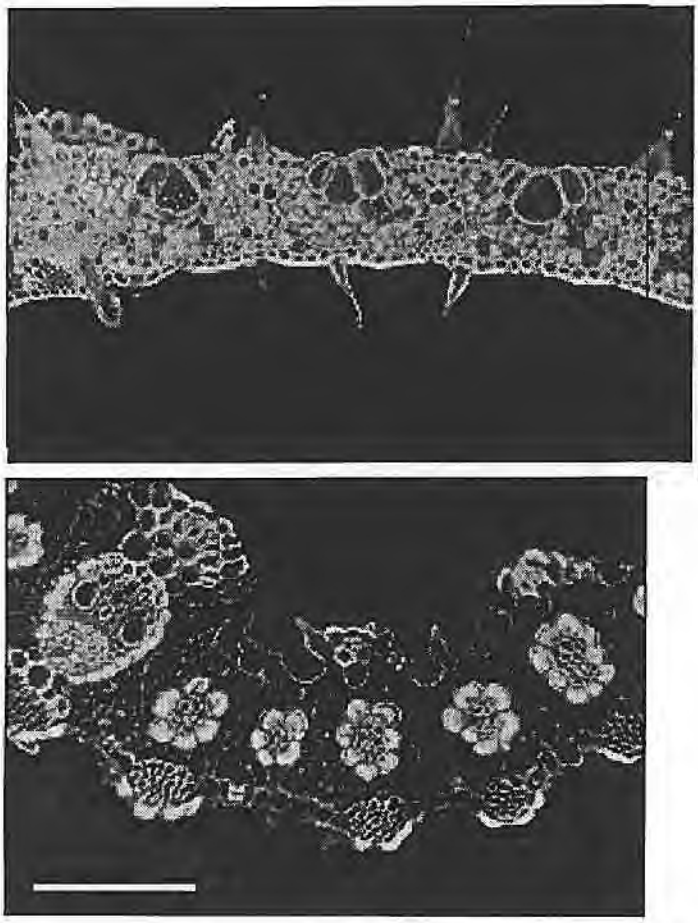

Figure 2.5 Rubisco can be localised in transverse sections of leaves by indirect immunofluorescent labelling where treated sections are viewed in conjunction with autofluorescence controls. Tissues such as bundle sheath extensions and epidermes fluoresce naturally, and such emission has to be 'substracted' from present images. Considering (a), all chloroplasts in this C_3 grass leaf (*Microlaena stipoides*) show a strong yellow fluorescence, indicating general distribution of Rubisco, and hence operation of the PCR cycle. By contrast, in (b), the C_4 grass (*Digitaria brownii*) has restricted Rubisco to bundle sheath cells. In that case, mesophyll cells are devoid of Rubisco, fixing CO_2 via the action of phosphoenolpyruvate carboxylase into a four-carbon acid which moves to bundle sheath cells, there providing CO_2 for subsequent refixation via Rubisco and the PCR cycle Scale bar is 100 μm (see Colour Plates xx and xx)
(Original light micrographs courtesy Paul Hattersley)

fluorochrome (fluorescein isothiocyanate) is applied to the preparation. This fluorochrome binds specifically to the rabbit antibodies and fluoresces bright yellow wherever Rubisco is located (blue light excitation using an epifluorescence light microscope).

In the C_3 grass *Microlaena stipoides* (Figure 2.5a), all chloroplasts are fluorescing bright yellow and this indicates wide distribution of Rubisco throughout mesophyll tissue. By contrast, only bundle sheath cells are equipped with Rubisco in the C_4 grass *Digitaria brownii* (Figure 2.5b).

These two native Australian grasses co-occur in the ACT but contrast in relative abundance. *M. stipoides* (weeping grass) is common in dry sclerophyll woodlands throughout southeast temperate Australia, whereas *D. brownii* (cotton panic grass) in the ACT is at the southern end of its distribution, being far more abundant in subtropical Australia and, in keeping with its C_4 physiology, especially prevalent in semi-arid regions.

C_4 energetics

One disadvantage of the C_4 pathway is that an energy cost is incurred by C_4 plants to run the CO_2 'pump'. This is due to the ATP required for recycling PEP (Figure 2.3 and Hatch 1988). Under ideal conditions five ATP and two NADPH are required for every CO_2 fixed in C_4 photosynthesis (two ATP are required to run the CO_2 pump). From the previous section, the C_4 pathway is obviously energetically more expensive than the C_3 pathway in the absence of photorespiration. However, at higher temperatures the ratio of RuBP oxygenation to carboxylation is increased and the energy requirements of C_3 photosynthesis can rise to more than five ATP and three NADPH per CO_2 fixed in air (for these calculations see Edwards and Walker 1983, and Hatch 1988).

Representative light response curves for photosynthesis in C_3 cf. C_4 plants (Figure 2.6) can be used to demonstrate some of these inherent differences in photosynthetic attributes. At low temperature (10°C in Figure 2.6) a C_3 leaf shows a steeper initial slope as well as a higher value for light-saturated photosynthesis. By implication, quantum yield is higher and photosynthetic capacity is greater under cool conditions. In terms of carbon gain and hence competitive ability, C_3 plants will thus have an advantage over C_4 plants at low temperature and especially under low light.

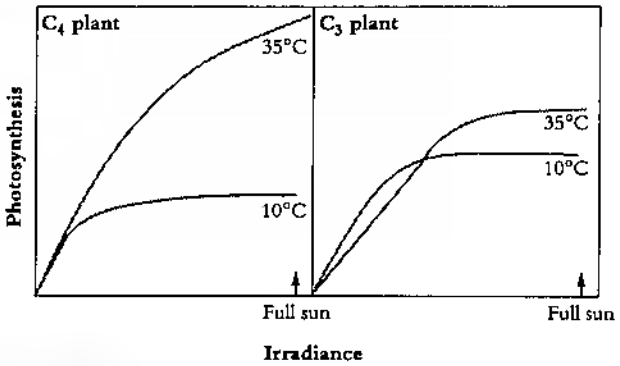

Figure 2.6 Generalised light response curves for leaf photosynthesis show that C_4 plants assimilate comparatively faster at high temperature (35°C), but that C_3 plants are advantaged at low temperature (10°C). Photorespiration increases with temperature, and is largely responsible for this contrast. C_4 plants are equipped with a CO_2-concentrating device in their bundle sheath tissue which both enhances Rubisco's performance at that location, and forestalls photorespiratory loss
(Original drawings coustesy M.D. Hatch)

By contrast, under warm conditions (35°C, upper curves in Figure 2.6) C_4 photosynthesis in full sun greatly exceeds C_3, while quantum yield (inferred from initial slopes) remains unaffected by temperature. Significantly, C_3 plants show a reduction in quantum yield under warm conditions (compare 10°C and 35°C curves; right side of Figure 2.6). At 35°C C_3 plants also show lower rates of light-saturated assimilation compared with C_4 plants. Increased photorespiratory losses from C_3 leaves at high temperature are responsible (Section 2.3). C_4 plants will thus have a competitive advantage over C_3 plants under warm conditions at both high and low irradiance.

2.1.6 Crassulacean acid metabolism (CAM)

A further adaptation to high temperature and in particular arid conditions is crassulacean acid metabolism (CAM) photosynthesis. Compared with the anatomical specialisation and *spatial* separation of biochemical function in C_4 plants, CAM photosynthesis does not require anatomical differentiation but instead involves a *temporal* separation of an *in situ* biochemical function. CAM is essentially an adaptation to reduce water loss through stomata by *reversing* the diurnal rhythm of CO_2 fixation. Typically, CAM plants are equipped with fleshy assimilatory organs (commonly phyllodes or cladodes) and include the majority of cacti and orchids as well as many salt-tolerant succulents (such as the ice plant *Mesembryanthemum crystallinum*) and pineapple. Whereas C_4 plants have a biochemical CO_2 pump, CAM plants operate more like a biochemical storage battery. During the night-time when the heat load is low and atmospheric water vapour pressure relatively high, stomata open, admitting CO_2, which is fixed by PEP carboxylase in much the same way as in C_4 photosynthesis. The C_4 product (usually malate) is stored in vacuolar compartments of these fleshy organs until the daytime. Malate is then decarboxylated to provide CO_2 for Rubisco (reviewed by Winter 1985). This tight cycle of malic acid storage and breakdown, often called 'acidification' and 'deacidification', is shown schematically in Figure 2.7 along with a simplified version of the CAM pathway.

Historically, the discovery of CAM plants can be attributed to this cyclical acidification/deacidification. In a letter to the Linnean Society in 1813 Benjamin Heyne wrote 'the leaves of the...plant called by Mr Salisbury *Bryophyllum calycinum*, which on the whole have an herbaceous taste, are in the morning as acid as sorrel, if not more so. As the day advances, they lose their acidity and are tasteless about noon...' (a more detailed account appears in Walker 1992). *B. calycinum* is, of course, a CAM plant and the acid taste is due to the build up of malic acid at night. However, despite these early observations, it took another 150 years to unravel the complexities of the CAM pathway.

Because the primary steps of carbon fixation by CAM plants occur in darkness, PEP synthesis and energy supply (in the form of ATP and reducing power) are closely linked to respiration plus breakdown of stored carbohydrates made during the previous photoperiod. Simplified in Figure 2.7, the CAM pathway relies on starch as a 'storage battery' of light-derived energy for subsequent PEP carboxylation in darkness. Malate stored in vacuolar compartments from night-time fixation is a carbon store that yields CO_2 in daytime.

Unlike C_4 plants, which have some of the highest growth rates of all land plants (Hatch 1988), CAM plants achieve rather meagre rates of photosynthesis and suffer a yield penalty as a result. Moreover, their modified pathway of photosynthesis with temporal separation of photochemical and biochemcial functions incurs an energetic cost of between 5.5 and 6.5 ATP and two NADPH per CO_2 fixed (Walker 1992). Compare this with a requirement of only three ATP (and two NADPH) per CO_2 fixed during C_3 photosynthesis in low oxygen.

Restrictions on inward diffusion of ambient CO_2 via sparse stomata and slow progress between decarboxylation and fixation sites through an extensive liquid phase of assimilatory tissue world place further constraints on carbon gain. Some relativities for C_3, C_4 and CAM gas exchange are summarised in Table 2.1. Potentially greater rates of assimilation by C_4 plants put that group at an advantage in terms of biomass gain and water use efficiency in daytime. For a given stomatal conductance, transpiration by C_3 and C_4 would be

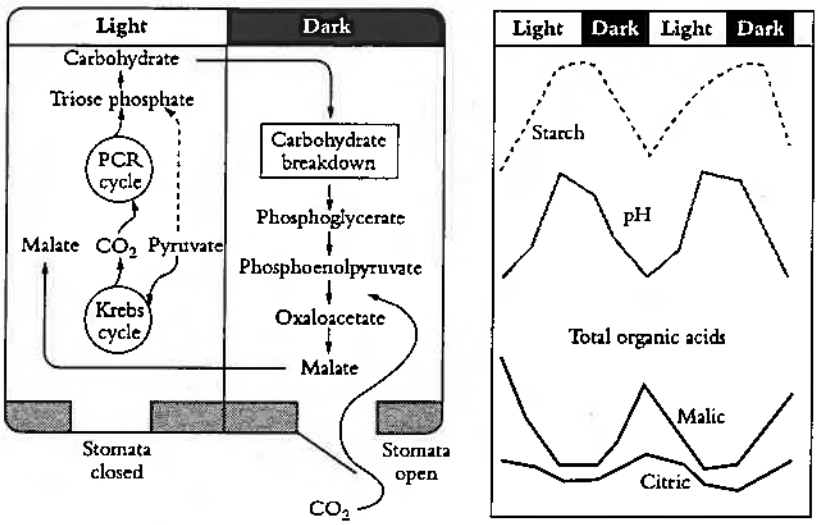

Figure 2.7 Crassulacean acid metabolism (CAM) is a photosynthetic adaptation to dry conditions and represents a 'survival option'. Stomata open at night-time allowing CO_2 entry and incorporation into a malate pool in mesophyll vacuoles. The next day, malate is metabolised to release CO_2 which is refixed by Rubisco while stomata remain closed
(Based on Walker 1992)

Table 2.1 Photosynthesis and leaf conductances in C_3, C_4 and CAM plants. Tr ratio (transpiration ratio) is expressed as mass of water transpired per unit mass of CO_2 assimilated.

Mode	Photosynthesis μmol CO_2 m^{-2} s^{-1}	Stomatal mol m^{-2} s^{-1}	Mesophyll mol m^{-2} s^{-1}	Tr ratio $H_2O\uparrow/CO_2\downarrow$
C_3	12.5–25.0	0.8–0.08	0.13–0.04	450–600
C_4	18.5–50.0	0.5–0.25	0.40–0.20	250–350
CAM light	1.85–12.5	0.06–0.04	0.02–0.01	150–600
dark	6.25–9.25	0.20–0.04	0.40–0.20	25–150

(Derived from generalised values of Szarek and Ting 1975)

comparable, but the greater CO_2-scavenging capacity of C_4 plants makes them more water efficient (greater inward flux of CO_2 for a given outward flux of H_2O). At night, CAM plants achieve further improvement in water use efficiency because CO_2 uptake is then combined with much reduced transpiration.

Table 2.1 emphasises adaptive features of C_3, C_4 and CAM photosynthesis. Light-saturated rates of photosynthesis in C_4 plants can be up to twice those in C_3, even though maximum stomatal conductance is commonly somewhat lower. By contrast, C_4 plants achieve much higher mesophyll conductance (a consequence of their remarkable CO_2-scavenging ability), and water use efficiency during photosynthesis is consequently enhanced (i.e. transpiration ratio is lower). Daytime assimilation by CAM plants can occur when moisture is abundant, and is analogous to C_3 photosynthesis with maximal rates comparable to lower values of C_3 plants. C_3 engagement by CAM plants diminishes as moisture stress intensifies, and in full CAM mode night-time assimilation assumes prominence. In that condition, PEP carboxylase is responsible for initial fixation with mesophyll conductance comparable to that of a C_4 plant. Water use efficiency is, however, much greater due to lower evaporative demand. Under extreme conditions, the night-time transpiration ratio in CAM plants can be an order of magnitude lower than in C_4 plants (right-hand column, Table 2.1).

Notwithstanding stomatal restrictions on CO_2 assimilation, frugal use of water rather than high rates of carbon gain would have been the primary driving variable for evolution of CAM plants. In this context, CAM photosynthesis is more of a 'survival option' where slow assimilation is an acceptable trade-off for a water-retentive physiology. The spectacular success of CAM photosynthesis in arid zones and dry habitats worldwide confirms this principle (discussed further in Section 16.5).

2.1.7 Submerged aquatic macrophytes (SAM)

Vascular plants often inhabit regions subject to tidal submergence while others carry out their entire life cycle under water. Examples of common submerged aquatic macrophytes are pond weeds and seagrasses. Once again, an evolutionary selective pressure for these plants has been availability of CO_2. Low levels of dissolved CO_2 are common in both inland and marine waters, particularly at more alkaline pH. In more productive inland lakes, CO_2 content can vary enormously, requiring considerable flexibility in the actual mode of carbon acquisition. At high pH, HCO_3^- becomes the more abundant form of inorganic carbon, whereas dissolved CO_2 will predominate at low pH (Section 19.3). Consequently, when SAM plants evolved from their C_3 progenitors on land, there was some adaptive advantage in devices for CO_2 accumulation because CO_2 rather than HCO_3^- is substrate for Rubisco. The nature of this 'CO_2 pump' and the energetics of carbon assimilation are not fully characterised in SAM plants but considerable CO_2 concentrations do build up within leaves, enhancing assimilation and suppressing photorespiration (Badger 1987, and discussed further in section 19.3).

Photosynthetic carbon gain — summary

Regardless of photosynthetic mode, and despite catalytic limitations, Rubisco is ubiquitous and remains pivotal to carbon gain in our biosphere. As a corollary, carbon loss via photorespiration is an equally universal feature of C_3 leaves, and the evolution of devices that overcome such losses have conferred significant adaptive advantages to C_4, CAM and SAM plants. Surprisingly, the biochemical sources for such massive dissipation of fixed carbon were not identified until biochemists combined forces in the early 1960s with leaf physiologists who were equipped with infrared CO_2 analysers. An historic account is given in Section 2.3.

2.1.8 Metabolite flux and organelle transporters

Integration of photosynthetic metabolism between compartments and maintenance of discrete environments within organelles require controlled movement of substances across membranes. This control is provided by an array of highly specific transport proteins which span the lipid bilayer of membranes. These transporters act as gatekeepers determining which substances may enter or leave, how fast they may move, and whether their entry involves an exchange of metabolites or an input of energy.

(a) Chloroplasts

Chloroplasts of higher plants are bounded by a double membrane known as the chloroplast envelope (Section 1.3). The two membranes of the envelope are separated by an average distance of only 6 nm, and between them is a small metabolic compartment known as the intermembrane space. Suspended within the chloroplast envelope there is a third, highly convoluted and protein-rich membrane system (thylakoid membranes) which delimits a separate metabolic compartment: the intrathylakoid space or lumen. The ground substance of chloroplasts (stroma) represents the third and largest compartment of chloroplasts (Section 1.3).

Some of the largest fluxes of metabolites in plants cross chloroplast membranes. In the intrathylakoid space, a continuous supply of water is required to sustain light-driven oxidation of water by photosystem II (PS II). The products of this process, protons and O_2, must also be continuously released across the thylakoid membrane and beyond. CO_2 is reduced within the stroma by the PCR cycle and incorporated into triose phosphates, starch, fatty acids, amino acids and terpenoids. These synthetic events are sustained by metabolite fluxes across the three membranes of the chloroplast. Oxygen is also reduced in the stroma in the oxygenase reaction catalysed by the enzyme ribulose-1,5- bisphosphate carboxylase/oxygenase (Rubisco). One product of this reaction, 2-phosphoglycolate, is dephosphorylated and exported from stroma to cytoplasm where it is processed by reactions of the photorespiratory cycle. On balance, however, illuminated chloroplasts are O_2 producers, and O_2 must cross the chloroplast envelope to be used in mitochondrial electron transport or else return to the atmosphere.

Not all metabolites need cross chloroplast membranes by means of a transporter protein. Small uncharged molecules such as O_2, H_2O and CO_2, as well as hydrophobic molecules such as lipids, can cross by simple diffusion. Some monocarboxylic acids, such as acetate, can also cross the chloroplast membranes by diffusion. While simple diffusion of these molecules may occur at thylakoid membranes and across the inner membrane of chloroplast envelopes, facilitated diffusion is probably the predominant process mediating the flux of these and other metabolites across the outer membrane of those envelopes. This outer membrane contains a pore protein (a channel) which is non-specific and allows the passage of molecules up to about 3 nm in size (equivalent to a molecular weight of about 10 000). The inner membrane, in contrast, contains an array of specific translocators that control the flow of metabolites between cytosol and stroma.

Phosphate translocator

The most common transporter in the inner membrane is the phosphate/triosephosphate (3-phosphoglycerate) translocator, commonly known as the phosphate translocator (Figure 2.8). This antiport mediates the export of reduced carbon, in the form of triose phosphates, from the stroma into the intermembrane space, from which it can diffuse relatively freely into the cytosol. Most of the triose phosphates are used in synthetic reactions such as sucrose synthesis, but some are used in degradative reactions such as those of glycolysis and respiration. In C_3 plants, the phosphate translocator catalyses a strict counter-exchange involving inorganic phosphate and phosphate molecules attached to the end of a three-carbon chain (e.g. triose phosphates, 3-PGA). During the day the main exchange process catalysed by the phosphate translocator is the export of triose phosphate for sucrose synthesis and the import of inorganic phosphate for ATP synthesis from ADP (C_3 chloroplast in Figure 2.8).

Different forms of the phosphate translocator are found in different types of plants and in different tissues within plants. In C_4 plants there are two different forms of the phosphate translocator which differ from the C_3 translocator in their ability to transport phosphoenolpyruvate. One form of the C_4 translocator is located in bundle sheath cell chloroplasts and the other one in mesophyll cell chloroplasts. Both forms transport triose phosphates, 3-PGA, inorganic phosphate and phosphoenolpyruvate, but the ability of the bundle sheath translocator to transport 3-PGA and phosphoenolpyruvate is lower than that of the mesophyll translocator. This difference reflects the major metabolic fluxes sustained by the two forms of the translocator.

In mesophyll cells of C_4 plants, phosphoenolpyruvate, which is synthesised in the stroma from imported pyruvate, is exported in exchange for inorganic phosphate to the cytosol where it is used by phosphoenolpyruvate carboxylase to fix CO_2 (C_4 mesophyll chloroplast in Figure 2.8). In the bundle sheath chloroplasts of certain C_4 plants (e.g. maize), relatively rapid 3-PGA–triose phosphate exchange is catalysed by the phosphate translocator. These chloroplasts lack PSII and thus the ability to reduce phosphoglycerate to triose phosphate. Phosphoglycerate is exported to the mesophyll chloroplasts for reduction and returned to the bundle sheath in the form of triose phosphate, which is used largely for the PCR cycle.

Plants with crassulacean acid metabolism (CAM) contain a chloroplast phosphate translocator which, similar to that of C_4 plants, has a relatively high ability to transport phosphoenolpyruvate. During the day, the main flux sustained by the phosphate translocator is the exchange of 3-PGA and phosphoenolpyruvate. Phosphoenolpyruvate is synthesised in the stroma and exported to the cytosol where it is converted into 3-PGA. The 3-PGA is, in turn, taken up by the chloroplast and used for starch synthesis (CAM chloroplast in Figure 2.8). The carbon source for phosphoenolpyruvate synthesis is malate which, after release from the vacuole, is decarboxylated and converted into pyruvate. The pyruvate enters the chloroplast, by means of a specific H^+/pyruvate or Na^+/pyruvate symport, where it is converted into phosphoenolpyruvate. A similar pyruvate translocator has been found in chloroplasts of C_4 mesophyll cells, some C_3 plants and the bundle sheath cells of some C_4 plants.

The phosphate translocator also catalyses triose phosphate–inorganic phosphate exchange in CAM plants. At night

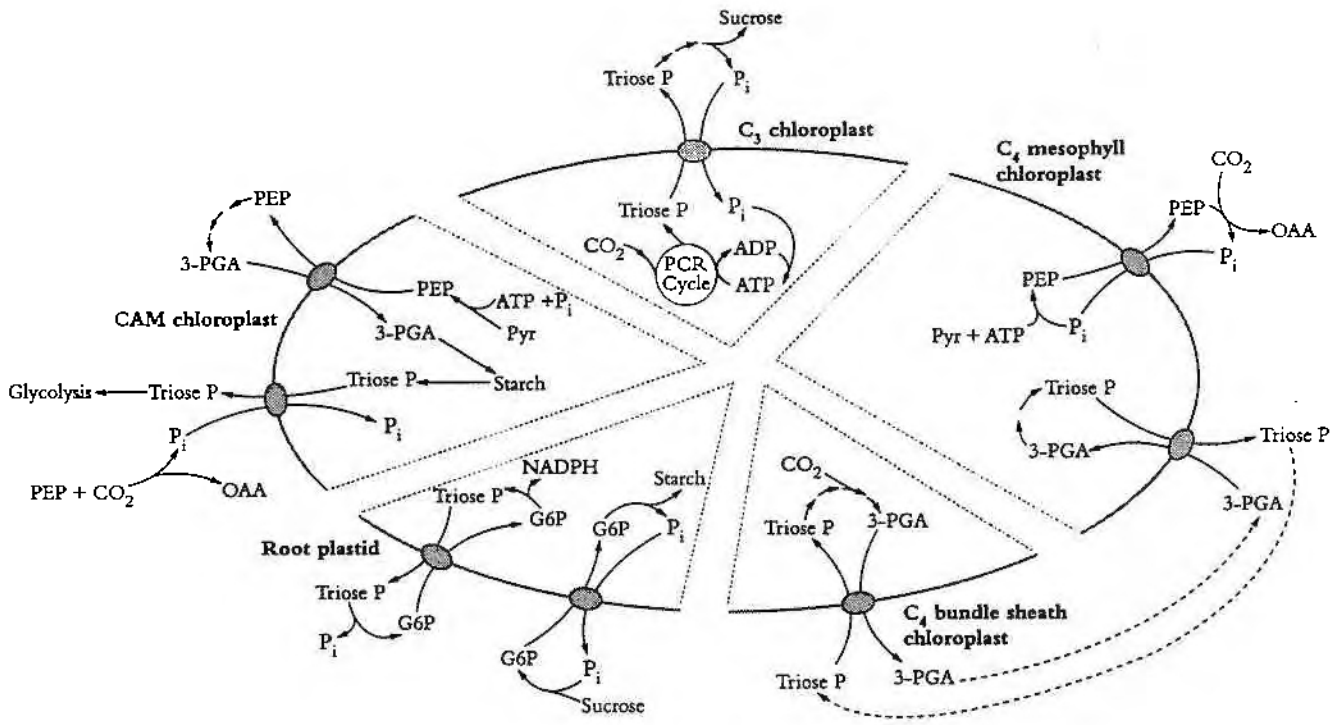

Figure 2.8 Phosphate translocators in plastids from different types of plants and tissues. In C_3 chloroplasts, the main function of the phosphate translocator is in exporting triose phosphate (triose P) to the cytosol where it is used mainly for sucrose synthesis. During the day, triose phosphate is produced by the photosynthetic carbon reduction (PCR) cycle.

Chloroplasts from the leaves of C_4 plants contain two forms of the phosphate translocator, one in the bundle sheath and the other in the mesophyll cells. The mesophyll translocator mediates phosphoenolpyruvate (PEP) export for use in CO_2 fixation. In bundle sheath chloroplasts of certain C_4 plants, 3-phosphoglycerate (3-PGA) is exported for reduction to triose phosphate in mesophyll cell chloroplasts.

The phosphate translocator in chloroplasts from plants with crassulacean acid metabolism (CAM) mediates PEP export in the daytime and triose P export at night. In contrast, the phosphate translocator in root plastids mediates the exchange of glucose-6-phosphate (G6P) and triose P. This exchange is important for the operation of the oxidative pentose phosphate pathway. G6P exchange for inorganic phosphate (P_i) is important in carbon import for starch synthesis. OAA = oxaloacetate
(Original drawing courtesy Ian Woodrow)

starch is degraded to triose phosphates, which are exported from chloroplasts for production of phosphoenolpyruvate (CAM chloroplast in Figure 2.8). PEP is the substrate for phosphoenolpyruvate carboxylase, an enzyme catalysing CO_2 fixation to form oxaloacetate. This metabolite is then converted into malate which is stored in the vacuole for use during subsequent daytime (Figure 2.7).

Despite little research on the phosphate translocators of other types of plastids, different forms are known to occur in root plastids, amyloplasts and chromoplasts. The main function of root plastids is the reduction of nitrite for which energy is supplied by the oxidative pentose phosphate pathway. Because these plastids do not have the enzyme fructose-1,6-bisphosphatase, operation of the oxidative pentose phosphate pathway requires the exchange of stromal triose phosphate for cytosolic glucose-6-phosphate (see root plastid in Figure 2.8). Accordingly, this root plastid translocator has been shown to have a relatively high ability for transporting glucose-6-phosphate.

Dicarboxylate translocators

At least two translocators mediate the exchange of a range of dicarboxylates across the inner membrane of chloroplasts.

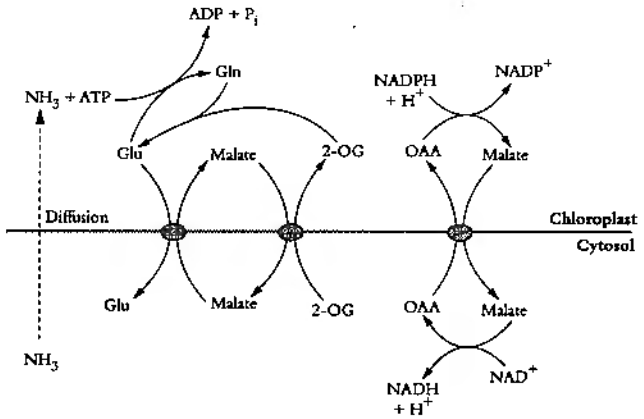

Figure 2.9 Dicarboxylate translocators on the inner membrane of chloroplasts have at least two important metabolic functions. A malate/oxaloacetate (OAA) translocator facilitates the export of reducing equivalents to the cytosol. NADPH is one of the products of the photosynthetic electron transport chain in chloroplasts. Two dicarboxylate translocators are involved in ammonia assimilation during photorespiration. In this process, ammonia is incorporated into glutamate (Glu), the production of which is sustained by 2-oxoglutarate (2-OG) import from the cytosol. Glutamine (Gln) and 2-oxoglutarate are substrates in a reaction that produces two molecules of glutamate. Of these, one is used for subsequent ammonia assimilation and one is exported in exchange for malate
(Original drawing courtesy Ian Woodrow)

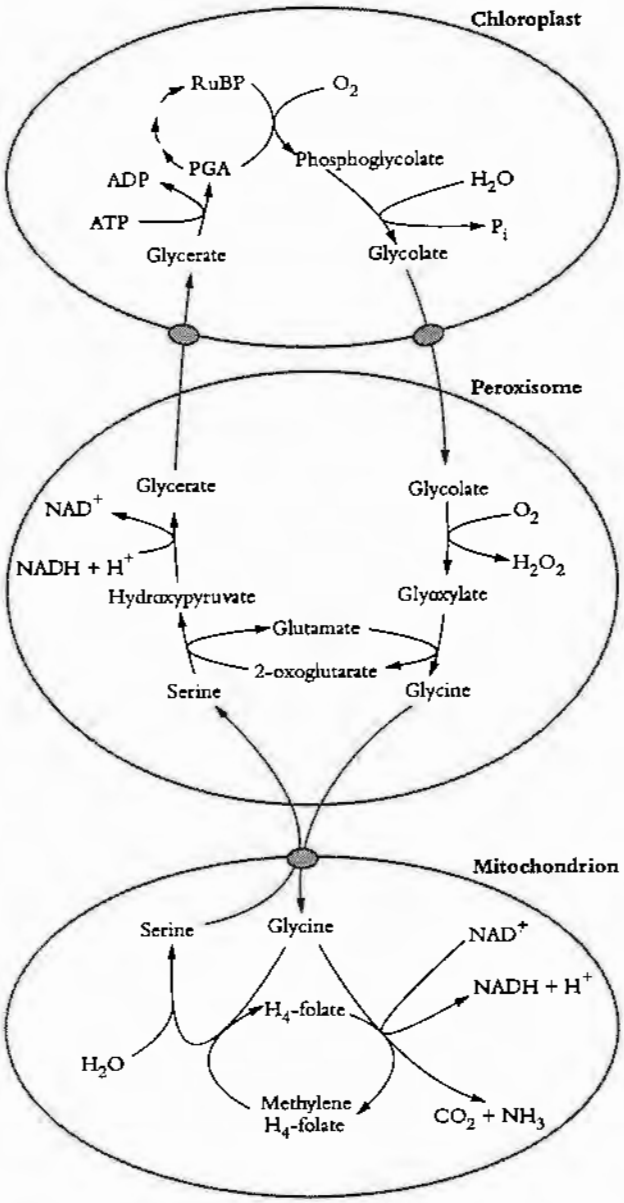

Figure 2.10 The photorespiratory carbon oxidation (PCO) cycle involves movement of metabolites between chloroplasts, peroxisomes and mitochondria. Transport of glycerate and glycolate across the inner membrane of chloroplasts may involve separate translocators as shown here, or it may involve a single translocator that exchanges two glycolate molecules for one molecule of glycerate. Transport of metabolites across the peroxisomal membrane most likely occurs through unspecific channel proteins, similar to those in the outer membranes of mitochondria and chloroplasts. These outer membranes are not included in this diagram. Mitochondria take up two molecules of glycine and release one molecule of serine. A specific translocator most probably mediates the exchange of these amino acids
(Original drawing courtesy Ian Woodrow)

They include malate, oxaloacetate, 2-oxoglutarate, aspartate, succinate, glutamate and glutamine (Figure 2.9). These translocators play a key role in two major metabolic processes, namely (1) the photorespiratory nitrogen cycle, and (2) export of reducing equivalents from chloroplasts. During photorespiration (Figure 2.10) ammonia is released by mitochondria and diffuses into chloroplasts (Figure 2.9) where it is incorporated into glutamate. Production of glutamate, which is catalysed by glutamine synthetase and glutamate synthase, requires a supply of 2-oxoglutarate from the stroma. Exported glutamate is not exchanged directly for 2-oxoglutarate. Rather, glutamate is exported in exchange for malate by the dicarboxylate translocator, and the malate is in turn exported in exchange for 2-oxoglutarate by a specific translocator (Figure 2.5.9) which cannot transport glutamate. There is therefore no net malate flux across the chloroplast envelope during this process.

A second dicarboxylate translocator in the inner membrane of chloroplasts mediates a specific oxaloacetate–malate exchange (Figure 2.9). Export of malate, subsequent oxidation to oxaloacetate in the cytosol, and subsequent import of oxaloacetate into chloroplasts for reconversion to malate facilitates a supply of reducing equivalents to the cytosol and peroxisomes. A malate/oxaloacetate translocator is also present in C_4 plants where it mediates the uptake of oxaloacetate formed by phosphoenolpyruvate carboxylase into mesophyll chloroplasts where it is reduced to malate. This is an important part of the C_4 cycle.

Glycolate/glycerate translocator

In C_3 plants, the rate of oxygenation catalysed by Rubisco, and thus the rate of photorespiration, is generally about one-third the rate of carboxylation. Phosphoglycolate production in the stroma is thus one of the largest metabolic fluxes in plants (Figure 2.10) and such flux is greatly facilitated by the close proximity of chloroplasts, peroxisomes and mitochondria. Indeed, these organelles are often contiguous (Figure 2.11).

Phosphoglycolate is dephosphorylated in the stroma and then exported to the cytoplasm by a specific translocator. For every two glycolate molecules exported, one molecule each of CO_2 and glycerate are produced. The glycerate is trans-

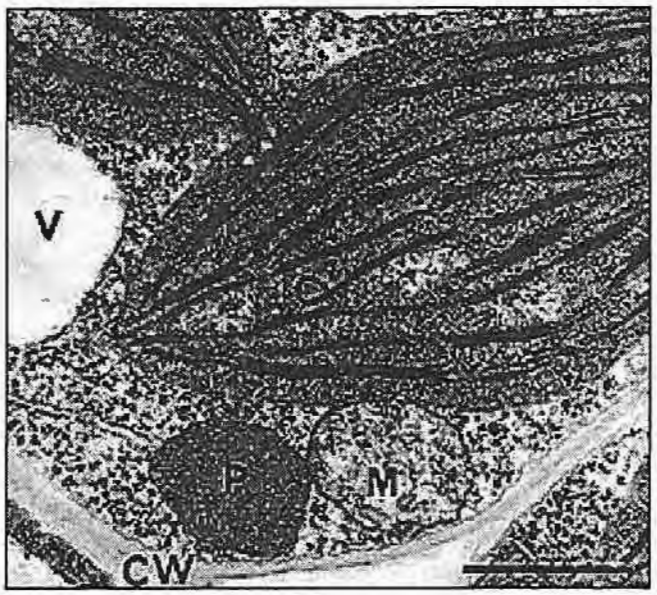

Figure 2.11 A transmission electron micrograph showing close juxtaposition of chloroplast (C), mitochondrion (M) and peroxisome (P) in a mesophyll cell of an immature leaf of bean (*Phaseolus vulgaris*). This group of organelles is held within a granular cytoplasmic matrix adjacent to a cell wall (CW) and includes a partial view of a small vacuole (V). Horizontal bar (lower right corner) = 1 μm
(Original electron micrograph courtesy Stuart Craig and Celia Miller)

ported into the chloroplast where it is phosphorylated (to produce 3-PGA) and used in the PCR cycle. Biochemical details of the exchange of two glycolate molecules for one glycerate molecule are not yet resolved. Either a single translocator mediates exchange of two glycolate molecules for one molecule of glycerate and one hydroxyl ion, or else separate glycolate and glycerate translocators exist (Figure 2.10).

ATP/ADP translocator

The inner membrane of a chloroplast envelope contains a translocator which catalyses the exchange of ATP and ADP (Figure 2.12). Chloroplasts are thus analogous to mitochondria, but differ in that ATP import is favoured. This translocator is especially active in developing chloroplasts of young leaves, providing ATP while photosynthetic capacity is still developing.

(b) Peroxisomes

Higher plants contain at least three specialised classes of peroxisomes which are defined according to their main enzyme content and metabolic function. The first class is glyoxisomes and these organelles are present in post-germinative seedlings and senescent organs. Their prime function is metabolism of storage lipids by means of a glyoxylate cycle. The second class of peroxisomes occurs in root nodules of some nitrogen-fixing legumes. These organelles contain urate oxidase which is involved in synthesis of ureides which represent the main nitrogenous compound exported from root nodules. The third class of peroxisomes is found in photosynthetically active tissues such as leaves and is an integral part of the photorespiratory cycle (Figures 2.10, 2.11). In addition to these three classes, there is a range of unspecialised peroxisomes isolated from a range of tissues including tubers, roots, fruits, petals and shoots that contain catalase and low levels of glycolate oxidase (general features of all classes of peroxisome).

Unlike chloroplasts and mitochondria, peroxisomes are encapsulated by only a single membrane (Figure 2.11). This membrane contains proteins, but no specific translocator has yet been identified. The membrane may contain a non-specific channel, similar to the one identified in rat liver peroxisomes and those in the outer membranes of chloroplasts and mitochondria. Such channels would provide a facilitated diffusion for exchange of metabolites between cytosol and peroxisomal compartments.

Metabolites in leaf peroxisomes are further compartmented by the process of metabolic channelling where enzymes of photorespiratory metabolism are organised into multi-enzyme complexes. In such systems, intermediates are not necessarily released into the aqueous phase of the peroxisome but 'passed' between active sites of different enzymes. This type of compartmentation protects a cell from toxic intermediates such as hydrogen peroxide and glyoxylate.

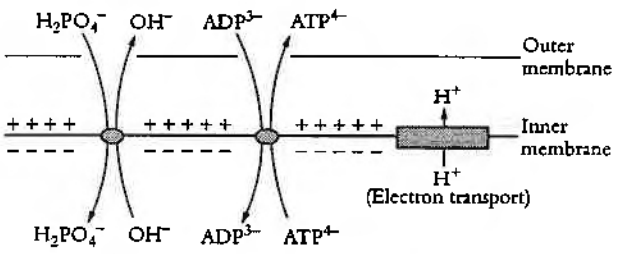

Figure 2.12 ATP synthesis in mitochondria requires a continuous supply of ADP and inorganic phosphate ($H_2PO_4^-$). ADP and phosphate are imported in exchange for ATP and an hydroxyl ion, respectively. These exchange processes, which are mediated by separate translocators, are favoured by the electrochemical potential difference across the inner membrane (indicated by the series of positive and negative charges). This difference results from proton translocation by the electron transport chain
(Original drawing courtesy Ian Woodrow)

(c) Mitochondria

All mitochondria house two metabolic compartments (Figure 2.22): first, an intermembrane space between outer and inner membranes of the mitochondrial envelope and, second, a matrix, held inside the highly convoluted inner membrane. As with the chloroplast envelope, outer and inner mitochondrial membranes differ in composition. The outer membrane is composed largely of lipids, whereas the inner membrane is composed of roughly equal proportions of proteins and lipids. These proteins comprise an electron transport system plus an array of specific translocators that regulate flow of metabolites to and from the metabolic pathways of the matrix. The outer membrane does not contain such an array of translocators; it contains a channel-forming porine protein which is non-specific and allows entry of molecules of up to about 2.5 nm in size (equivalent to a molecular weight of about 7000).

Not all metabolites require a translocator in order to cross the inner membrane of mitochondria. Small uncharged molecules such as CO_2, NH_3 and H_2O diffuse into and out of the mitochondria at relatively high rates. Moreover, certain amino acids and monocarboxylates can cross the inner membrane in their neutral form.

Enzymes catalysing reactions of the tricarboxylic acid cycle (TCA) cycle (Figure 2.23) reside within the mitochondrial matrix. This cycle, which requires a supply of pyruvate and malate from the cytosol, provides reducing equivalents to the electron transport chain for ATP synthesis and numerous substrates for the biosynthetic reactions in the rest of the cytoplasm. Enzymes in the mitochondrial matrix also feature in other major metabolic pathways including photorespiration, lipid metabolism and amino acid synthesis. As outlined below, the scale of these various metabolic functions and therefore the importance of respective metabolite translocators will vary according to organ function and growing conditions.

Amino acid translocators

In photosynthetic tissues and especially in C_3 plants, one of the largest metabolic fluxes sustained by mitochondrial metabolite translocators is that of photorespiration. As outlined above (Figure 2.10; see also Section 2.3), this process involves chloroplasts, peroxisomes and mitochondria. During these processes, referred to collectively as photorespiration, mitochondria take up two glycine molecules from the perox-

isomes and release one molecule each of serine, CO_2 and ammonia. A specific glycine translocator appears to catalyse exchange of two glycine molecules for one serine molecule and an hydroxyl ion. Neither CO_2 nor ammonia requires a translocator to cross the inner membrane.

While several other amino acids have been shown to enter mitochondria by diffusion across both membranes, there are a number of other specific translocator proteins on the inner membrane. These proteins transport glutamate, aspartate and proline. The exchange of amino acids across the inner membrane is important for protein synthesis and turnover within the mitochondria, for the interconversion of amino acids, and possibly for the exchange of reducing equivalents with the cytoplasm. There is, however, little evidence that amino acids are imported into mitochondria as substrates for the TCA cycle. One exception to this may involve proline import. Proline accumulates in plant cells when they are subject to especially water and cold stress. When the stress is removed, proline is rapidly metabolised in the mitochondria where it is ultimately converted to 2-oxoglutarate, a TCA cycle intermediate.

Adenine nucleotide and phosphate transport

A principal function of mitochondria is production of ATP. The enzyme responsible, F_1-ATPase, is located on the inner surface of the inner membrane (Figure 2.24). ATP synthesis therefore requires a continuous flow of ADP and phosphate across the inner membrane. ADP import and ATP export is catalysed by a specific translocator that exchanges ATP for ADP. The rate of this exchange is enhanced by a proton gradient across the inner membrane that favours export of the more negatively charged ATP molecule (Figure 2.12). Inorganic phosphate is transported separately, but the translocator for this metabolite is also located on the inner membrane and appears to catalyse the exchange of phosphate with an hydroxyl ion. As with ATP export, phosphate import is favoured by a proton gradient that exists across the inner membrane (Figure 2.12).

Pyruvate transport

The TCA cycle in the mitochondrial matrix generally requires a supply of pyruvate to generate reductants required for electron transport and ATP synthesis. Pyruvate, generated by glycolysis in the cytosol, is transported across the inner membrane by a specific translocator that catalyses an exchange of pyruvate (one negative charge) with an hydroxyl ion (one negative charge), thus maintaining electrical neutrality. Uncharged pyruvic acid can also diffuse across the inner membrane at appreciable rates. However, pyruvic acid has a relatively low pKa and consequently passive diffusion of this substance is probably not important under physiological conditions. Inside the matrix, pyruvate is oxidatively decarboxylated by the multienzyme pyruvate dehydrogenase complex to yield NADH, CO_2 and, especially important, acetyl CoA which then enters the TCA cycle.

Dicarboxylate translocators

Pyruvate is not and cannot be the only TCA cycle substrate (Figure 2.23). In almost all tissues, acetyl CoA entering the TCA cycle is not oxidised completely to CO_2. Rather, a significant proportion of the carbon (in the form of various intermediates) is removed from the cycle for biosynthetic reactions. Because the TCA cycle cannot catalyse the net synthesis of any intermediate, depletion of intermediates by the biosynthetic pathways must be balanced by an import of at least one intermediate. In most tissues, malate is the intermediate imported to replenish the TCA cycle.

Oxaloacetate and aspartate can also be imported to varying degrees. Once in the matrix, malate may be oxidised by the TCA cycle or converted to pyruvate or a combination of both processes. Malate is produced in the cytoplasm in the degradation of proteins or from phosphoenolpyruvate, an end-product of glycolysis.

Malate import is mediated by several translocators: first, a dicarboxylate translocator which exchanges malate for inorganic phosphate, malonate or succinate; second, a 2-oxoglutarate transporter which exchanges 2-oxoglutarate for malate, malonate, succinate and oxaloacetate, but not inorganic phosphate; third, a uniport protein that facilitates malate import. Because of a requirement for charge compensation (malate carries two negative charges), malate translocation by this uniport is probably coupled to oxaloacetate transport in the opposite direction by another uniport. By operating in synchrony, these two uniports could therefore act as an effective malate/oxaloacetate exchange translocator.

Malate/oxaloacetate exchange is especially important in green tissue where it plays a key role in sustaining photorespiration. Imported oxaloacetate is reduced using the NADH produced during glycine oxidation. Malate, the product of this reduction, is then exported to the peroxisome where its oxidation is linked to the reduction of β-hydroxypyruvate (Figure 2.10). A malate/oxaloacetate translocator therefore mediates export of reducing equivalents from the matrix.

Tricarboxylate translocators

There is evidence for several translocators capable of catalysing citrate transport across the inner membrane of mitochondria, but only one tricarboxylate translocator has been isolated and characterised. This translocator exchanges citrate and malate. However, there is a difference in charge between these two compounds. At physiological pH, citrate has three negative charges whereas malate has only two. A separate proton translocation by the electron transport chain is therefore required to restore charge balance.

Citrate is synthesised exclusively in mitochondria (Figure 2.23) and is exported to the cytosol for conversion to 2-oxoglutarate in reactions catalysed by aconitase and NADP-isocitrate dehydrogenase. A continuous supply of 2-oxoglutarate is required primarily for ammonia assimilation by chloroplasts in a reaction catalysed by glutamine synthetase. Citrate export and subsequent use in ammonia fixation is not needed to sus-

tain the relatively high rate of ammonia production associated with photorespiration. For this process, 2-oxoglutarate is produced in the peroxisomes as a product of photorespiration and imported into the chloroplast for ammonia assimilation. Photorespiration does not, therefore, result in an overall release of nitrogen.

(d) Vacuolar malate translocators and CAM photosynthesis

Malate transport from cytosol to vacuole across the tonoplast is mediated by at least two types of channel. One channel is involved in malate uptake. This channel opens when the pH gradient across the tonoplast is sufficient to allow for uptake of the negatively charged malate ion against a concentration gradient. This pH gradient constitutes an energy source for malate uptake and is generated by both ATP-dependent and pyrophosphate-dependent proton pumps which translocate protons from cytsol to vacuole. A second channel mediates malate efflux and also opens and closes in response to changes in pH gradient across the tonoplast. Malate efflux, however, generally occurs down a concentration gradient.

Some of the largest fluxes of malate into and out of vacuoles have been measured in CAM plants where CO_2 is fixed at night via PEP carboxylase (Figure 2.7). Fixed CO_2 is incorporated into malate, which is then transported across the tonoplast and stored at a relatively high concentration in vacuoles. During the daytime, malate is released from vacuole to cytosol where it is decarboxylated. CO_2 released in this process is then fixed by the PCR cycle in chloroplasts.

2.2 C_4 subgroups

2.2.1 Evolution of the C_4 mode

Approximately 85% of all terrestrial plant species are C_3, plants, while about 10% are CAM plants and are usually found in highly xeric sites (deserts, epiphytic habitats). The remainder are C_4 plants, and these become more dominant with aridity. Naively, we could conclude that evolution of C_4 photosynthesis was a response to selection by high temperature and low water availability. More likely, a decline in atmospheric CO_2 concentration during past millennia provided an initial impetus.

One hundred million years ago (Mid-Cretaceous), atmospheric CO_2 was between 1500 and 3000 $\mu L\ L^{-1}$, or four to ten times post-industrial levels. Given such a large concentration of CO_2 at that time, photorespiration of C_3 plants was inhibited (Section 2.3) so that photosynthetic efficiency was higher than it is now. In addition, maximum photosynthetic rates were double twentieth century values, and the energy cost of photosynthesis would have been around three ATP and two NADPH per molecule of CO_2 fixed. However, as atmospheric CO_2 concentrations declined to approximately 250–300 $\mu L\ L^{-1}$, photosynthetic rates were halved, photorespiration increased substantially, photosynthetic efficiency declined and the energetic costs of photosynthesis increased to approximately five ATP and 3.2 NaDPH per CO_2 molecule fixed. Such events would have generated a strong selection pressure for genetic variants with increased carboxylation efficiency and increased photosynthetic rates.

Angiosperms have a higher relative specificity of Rubisco for CO_2 than ferns and mosses (see examples of other less evolutionarily advanced species in Figure 2.2). Such differences imply minor evolution in this highly conserved molecule of Rubisco and there is little variation between species of vascular plants. Consequently, alteration of Rubisco in response to a changing atmospheric CO_2 concentration has not been an option.

By contrast, evolution of a new photosynthetic pathway (C_4) has occurred independently and on several occasions in diverse taxa over 50 to 60 million years as CO_2 levels declined. The oldest identifiable fossils with pronounced bundle-sheath layers are seven million years old, although necessary metabolic pathways could have evolved earlier, prior to this adaptation in anatomy. C_4 plants are known to differ from C_3 plants in their discrimination against atmospheric $^{13}CO_2$, and shifts in the stable carbon-isotope signature of soil carbonate layers that reflect emergence of C_4 plants have been dated at 7.5 million years BP. By inference, C_4 photosynthesis evolved in response to a significant decline in atmospheric CO_2 concentration, from 1500–3000 $\mu L\ L^{-1}$ to about 300 $\mu L\ L^{-1}$. By evolving a CO_2^- concentrating mechanism, Rubisco in C_4 plants was then presented with an elevated partial pressure of CO_2 despite lower atmospheric CO_2. As a consequence, photorespiration was inhibited, maximum photosynthetic rates increased and energetic costs reduced.

2.2.2 Concentrating CO_2 in bundle sheath cells

C_4 photosynthesis calls for metabolic compartmentation which is in turn linked to specialised anatomy (Figure 2.3). Three variants of C_4 photosynthesis have evolved which probably derive from subtle differences in the original physiology and leaf anatomy of their C_3 progenitors.

CO_2 assimilation by all three subgroups of C_4 plants (Figure 2.13) involves five stages:

1. carboxylation of PEP in mesophyll cells, thereby generating four-carbon acids (malate and/or aspartate);
2. transport of four-carbon acids to bundle sheath (BS) cells;
3. decarboxylation of four-carbon acids to liberate CO_2;
4. re-fixation of this CO_2 via Rubisco within the bundle sheath, using the C_3 pathway;
5. transport of three-carbon acid products following decarboxylation back to mesophyll cells to enable synthesis of more PEP.

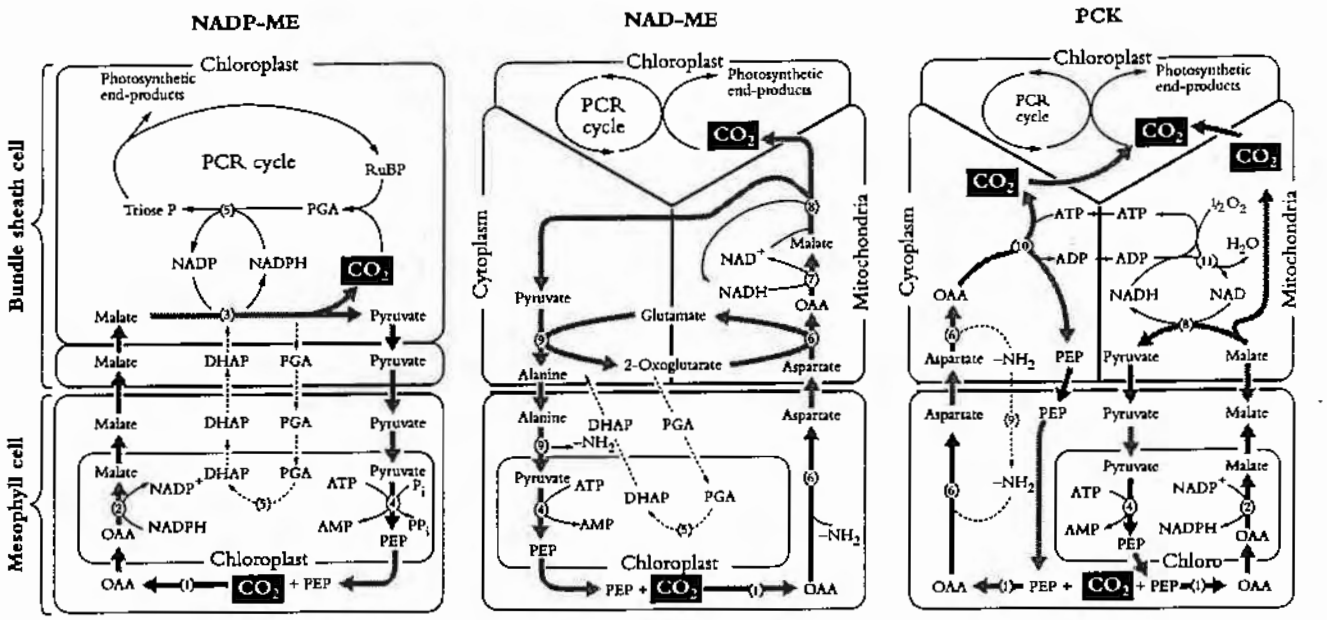

Figure 2.13 C_4 plants belong to one of three subgroups represented here (left to right) as NADP-ME, NAD-ME and PCK. Each subgroup has a distinctive complement and location of decarboxylating enzymes, and each differs with respect to metabolites transferred between mesophyll and bundle sheath. The path of carbon assimilation and intercellular and intracellular location of key reactions are shown for each of these biochemically distinct subgroups. Heavy arrows indicate the main path of carbon flow and associated transport of metabolites. Enzymes involved (numbers shown in paretheses) are as follows: (1) PEP carboxylase, (2) NADP malate dehydrogenase, (3) NADP malic enzyme, (4) pyruvate P_i dikinase (5) 3-PGA kinase and GAP dehydrogenase, (6) aspartate aminotransferase, (7) NAD malate dehydrogenase, (8) NAD malic enzyme, (9) alanine aminotransferase, (10) PEP carboxykinase, (11) mitochondrial NADH oxidation systems. In PCK-type C_4 plants, the PGA/DHAP shuttle would also operate between cells as indicated for NADP-ME and NAD-ME. Cycling of amino groups between mesophyll and bundle sheath cells involves alanine and alanine aminotransferase
(Original diagram courtesy Hal Hatch)

However, recognising some systematic distinctions in whether malate or aspartate was transported to bundle sheath cells, C_4 plants were further subdivided into three subgroups according to their four-carbon acid decarboxylating systems and ultrastructural features (Hatch *et al.* 1975). Members of each group contain high levels of either NADP malic enzyme (NADP-ME), phosphoenolpyruvate carboxykinase (PCK) or NAD malic enzyme (NAD-ME) (so designated in Figure 2.13). High NADP malic enzyme activity is always associated with higher NADP malate dehydrogenase activity, while those species featuring high activities of either of the other two decarboxylases always contain high levels of aminotransferase and alanine aminotransferase activities. As a further distinction, each of the decarboxylating enzymes is located in bundle sheath cells; NAD malic enzyme is located in mitochondria but phosphoenolpyruvate carboxykinase is not.

In all three subgroups, the primary carboxylation event occurs in mesophyll cytoplasm with PEP carboxylase acting on HCO_3^- to form oxaloacetate. However, the fate of this oxaloacetate varies according to subgroup (Table 2.2; Figure 2.13). In NADP-ME species, oxaloacetate is quickly reduced to malate in mesophyll chloroplasts using NADPH. By contrast, in NAD-ME and PCK species, oxaloacetate is transaminated in the cytoplasm, with glutamate donating the amino group, to generate aspartate. Thus, malate is transferred to bundle sheath cells in NADP-ME species and aspartate is transferred in NAD-ME and PCK species. The chemical identity of three-carbon acids returned to mesophyll cells varies accordingly.

Table 2.2 *C_4 plants belong to one of three subgroups which differ in identity and location of enzymes responsible for decarboxylation*

	Type of C_4 plant		
	NADP-ME	**NAD-ME**	**PCK**
Decarboxylating enzyme	NADP-dependent malic enzyme	NAD-dependent malic enzyme	Phosphenol-pyruvate carboxykinase
Location of decarboxylating enzyme	Chloroplast	Mitochondria	Cytoplasm
Main four-carbon acid moved to bundle sheath	Malate	Aspartate	Aspartate
Main three-carbon acid returned to mesophyll	Pyruvate	Alanine	Alanine/pyruvate

(Adapted from Hatch 1992)

Note also (Figure 2.13) that in NADP-ME species, only chloroplasts are involved in decarboxylation and subsequent carboxylation via the PCR cycle. By contrast, in NAD-ME and PCK species, chloroplasts, cytoplasm and mitochondria are all involved in moving carbon to the PCR cycle of bundle sheath chloroplasts. In NAD-ME and PCK species, aspartate arriving in bundle sheath cells is reconverted to oxaloacetate in either mitochondria (NAD-ME) or cytoplasm (PCK) (Table 2.2). Reduction and decarboxylation of oxaloacetate occurs in mitochondria of NAD-ME species and CO_2 is thereby released for fixation by chloroplasts of bundle sheath cells. In PCK species, oxaloacetate in the cytoplasm is decarboxylated by PEP carboxykinase, thereby releasing CO_2 for fixation in bundle sheath chloroplasts (Figure 2.13).

Transport of metabolites to bundle sheath cells

A rapid transfer of malate and aspartate to bundle sheath cells from mesophyll cells is required if the CO_2 concentration in bundle sheath cells is to stay high. A very high density of plasmodesmata linking bundle sheath cells to mesophyll cells facilitates this traffic. Consequently the permeability coefficient of C_4 bundle sheath cells to small metabolites such as four-carbon acids is about 10 times larger than that of C_3 mesophyll cells (Table 2.3). However, coupled with this need for a high permeability to metabolites moving into bundle sheath cells is a low permeability to CO_2 molecules so that CO_2 released through decarboxylation in the bundle sheath does not diffuse rapidly into mesophyll airspaces. For some species, a layer of suberin in the cell wall of bundle sheath-mesophyll junctions (suberin lamella) significantly reduces CO_2 efflux (Table 2.3).

Table 2.3 A high density of plasmodesmata significantly increases the permeability of bundle sheath cells to small metabolites such as aspartate and malate. Permeability to CO_2 is much reduced by a suberin layer in the walls of bundle sheath–mesophyll cell junctions. In NAD-ME types of C_4 plants, centripetal distribution of chloroplasts within bundle sheath cells helps restrict outward diffusion of CO_2

Plant type	Permeability coefficient (μmol min^{-1} (mg Chl)$^{-1}$ mM^{-1} for small metabolites	Permeability coefficient for CO_2
C_3	<0.3	>2000
C_4	2–5	≈ 15

(Adapted from Hatch 1992)

plants thus maintain a competitive advantage over C_3 plants in tropical locations, where average daily light receipt is much larger than in temperate zones, and associated with warmer conditions that also favour C_4 photosynthesis (Figure 2.6).

Given strong sunlight, warmth and seasonally abundant water, biomass production by C_4 plants is commonly double the rate for C_3 plants. Typically, C_3 plants produce 15–25 t ha^{-1} but C_4 plants easily produce 35–45 t ha^{-1}. Added to this superior light-saturated capacity, C_4 plants achieve higher nitrogen and water use efficiencies due to their CO_2-concentrating mechanism and absence of photorespiration. Accordingly, C_4

Centrifugal versus centripetal chloroplasts

Not all species contain a suberin layer, but all C_4 plants have a need to prevent CO_2 from diffusing quickly out of bundle sheath cells, so that the location of chloroplasts of bundle sheath cells becomes critical in those species lacking a suberin layer (Figure 2.14). Where species have a suberin layer, chloroplasts are located in a centrifugal position, that is, on the wall furtherest away from the centre of the vascular bundle lying in the middle of the bundle sheath (Figure 2.14E,F). In contrast, in those C_4 species lacking a suberin layer, chloroplasts are located centripetally, that is, on the wall closest to the centre of the vascular bundle lying within the bundle sheath (Figure 2.14A,B). Such a location would help restrict CO_2 diffusion from bundle sheath to mesophyll cells.

2.2.3 Regulation of C_4 photosynthesis

Fixation of CO_2 by C_4 plants involves the coordinated activity of two cycles in separate anatomical compartments (Figure 2.13). The first cycle is C_4 (carboxylation by PEP carboxylase), the second is C_3 (carboxylation by Rubisco). Given this biochemical and anatomical complexity, close regulation of enzyme activities is a prerequisite for efficient coordination.

PEP carboxylase, NADP malate dehydrogenase and pyuvate orthophosphate dikinase are all light regulated and their activities vary according to irradiance. NADP malate dehydrogenase is regulated indirectly by light via the thioredoxin system.

PEP carboxylase in C_4 plants exists in the same homotetramer in light- as in dark-adapted leaves. This is in marked contrast to CAM species where different forms exist in light- and dark-adapted leaves. In C_4 plants, PEP carboxylase has extremely low activity at night, thus preventing uncontrolled consumption of PEP. Such complete loss of activity in darkness is mediated via divalent metal ions, pH plus allosteric activators and inhibitors. As a consequence, and over a period of days, C_4 plants can increase or decrease PEP carboxylase in response to light regime.

2.2.4 Environmental physiology

C_4 species frequently occur in regions of strong irradiance. For example, the C_4 grasses of savannas of northern Australia are relatively unshaded because of the low tree density and sparse canopy. Light is abundant and since the CO_2 concentration inside C_4 leaves is high, a potentially high rate of light-saturated assimilation can be exploited. Most C_3 species reach light saturation in the range of one-eight to one-half full sunlight (Figure 2.6). In C_4 species, canopy assimilation might not become light saturated even in full sunlight. C_4

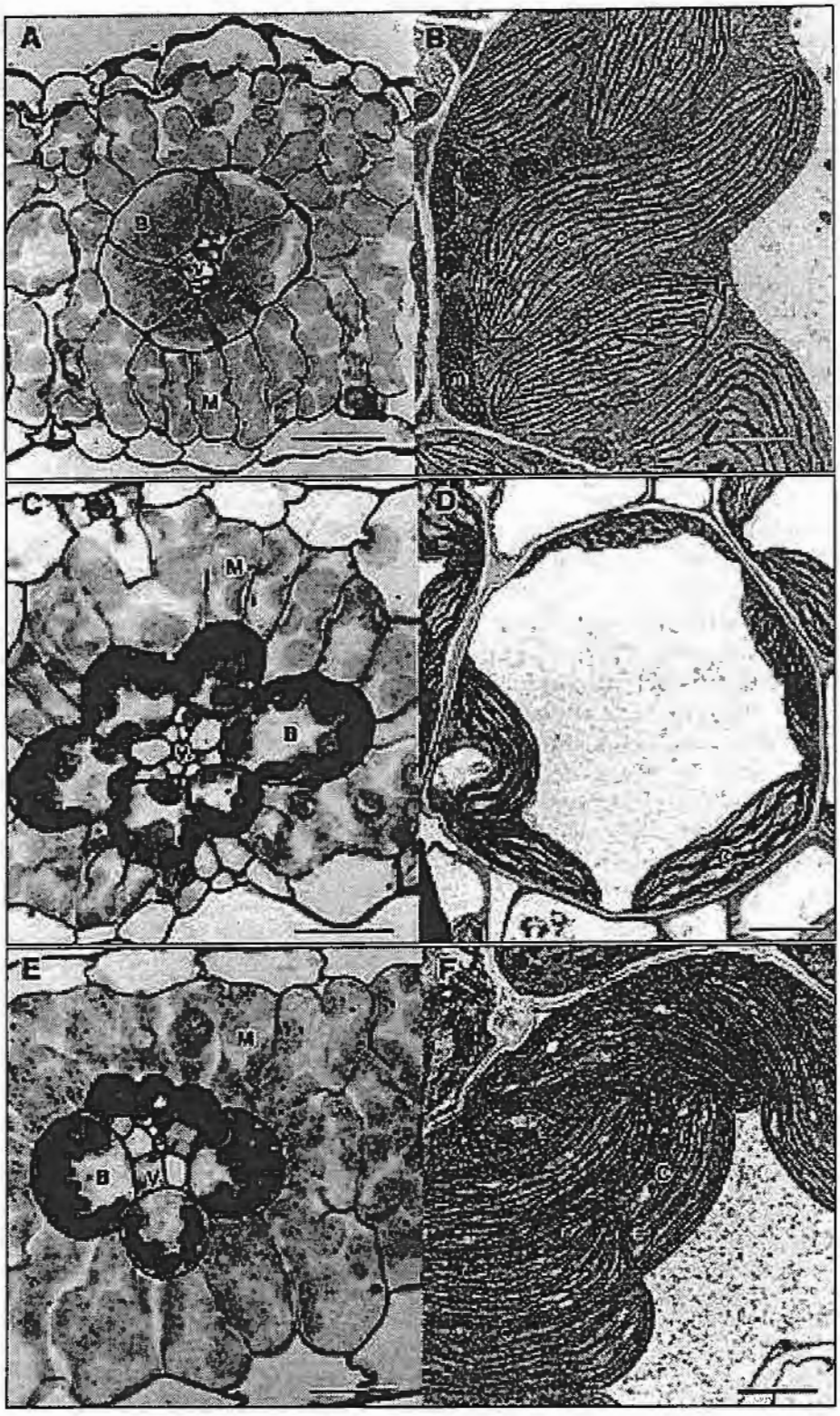

Figure 2.14 C_4 plants belong to one of three subgroups shown here in cross- section as light micrographs (left side) and electron micrographs (right side). Top to bottom, these subgroups are designated NAD-ME (A,B) PCK (C,D) and NADP-ME (E,F). Features common to all subgroups include a vascular bundle (V), bundle sheath (B), mesophyll tissue (M) and chloroplasts (C). See text and Hatch *et al.* (1975) for detailed explanation of subgroups.

Subgroup NAD-ME (A,B) is represented by *Amaranthus edulis* and shown bundle sheath cells with centripetally located chloroplasts containing small starch grains and surrounded by mesophyll cells. The accompanying electron micrograph of a cytoplasmic region of a bundle sheath cell shows chloroplasts and numerous large mitochondria. Scale bar in A = 50 μm; in B = 2 μm.

Subgroup PCK (C,D) is represented by *Chloris gayana* with chloroplasts arranged around the periphery of bundle sheath cells and adopting a centrifugal position. Mitochondria show well-developed internal membrane structures. Scale bar in C = 25 μm; in D = 3 μm.

Subgroup NADP-ME is represented by *Zea mays* where the bundle sheath contains centrifugally located chloroplasts with numerous starch grains, but lacking grana. Chloroplasts in adjacent mesophyll cells are strongly granal. Bundle sheath cells contain few mitochondria and these show only moderate development of internal membrane structures. Scale bar in E = 25 μm; in F = 2 μm

(Original micrographs courtesy Stuart Craig and Celia Millet)

plants are advantaged relative to C_3 plants in hot and nitrogen-poor environments with short growing seasons, hence their great abundance in wet/dry tropics such as Northern Territory savannas.

2.3 Photorespiration

During gas exchange by illuminated leaves, photosynthesis and respiration sustain bidirectional fluxes of the same two gases. In light, the balance of CO_2 and O_2 exchange represents the activity of both processes and to detect and measure the rates of each requires that they be separated. Moreover, respiratory output of CO_2 is also directly affected by light (Section 2.4), so that a further distinction needs to be made between 'dark' respiration during illumination, and 'photorespiration' *per se*. As outlined below, these processes are qualitatively distinct. Their separation necessitated some sophisticated measuring techniques, and their measurement led to some significant insights into leaf physiology.

2.3.1 Evidence for photorespiration

The most obvious demonstration that a net release of respiratory CO_2 occurs in light is the CO_2 compensation point. When air is recirculated over an illuminated leaf in a closed system, photosynthesis will reduce CO_2 concentration to a low level where fixation of CO_2 by photosynthesis is just offset by release from respiration. For many C_3 plants this compensation point is around 50 $\mu L\ L^{-1}$ but is markedly affected by oxygen, photon irradiance and leaf temperature (Egle and Schenk 1953; Tregunna *et al.* 1966; Zelitch 1966). Response to O_2 has some important implications and in low concentrations (1–2% O_2) the CO_2 compensation point is near zero (Figure 2.15) while net photosynthesis is increased (Tregunna *et al.* 1966).

Significandy, early researchers in this area had already noted that some tropical grass species appeared to have a compensation point at or close to zero CO_2, even in normal air (20% O_2). This was first reported for corn (*Zea mays*) (Meidner 1962; Forrester *et al.* 1966) and raised a very perplexing question as to whether these species even respired in light. However, we now know that C_4 photosynthesis is responsible (Section 2.2) and that C_4 plants have a CO_2-concentrating mechanism that forestalls photorespiration, resulting in a CO_2 compensation point close to zero.

A second line of evidence for leaf respiration in light was provided by a transient increase in release of CO_2 when leaves are transferred from light to dark (Figure 2.16). This 'post-illumination CO_2 burst' was studied extensively during the early 1960s by Gleb Krotkov and colleagues at Queens University (Kingston, Ontario) (Krotkov 1963). The intensity of this

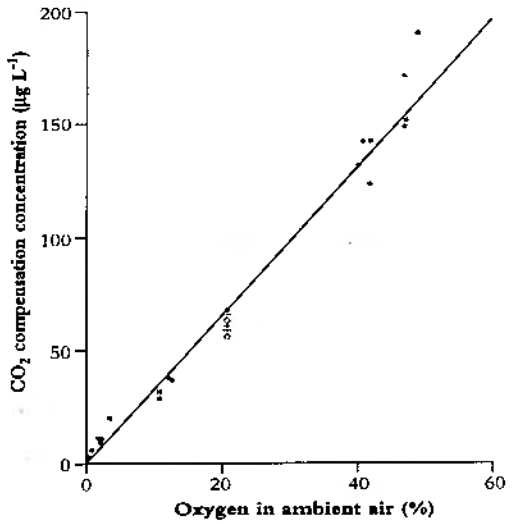

Figure 2.15 Illuminated (detached) tobacco leaves were held in a closed system of recirculating gas (initially 100 $\mu L\ L^{-1}$ CO_2 and 21% O_2) and allowed to equilibrate with ambient CO_2, thereby obtaining a CO_2 compensation point. O_2 levels were varied between 2% and 47% in subsequent experiments. The CO_2 compensation point at equilibrium showed a linear dependence on surrounding O_2 concentration. Data from two leaves have been combined (Based on Krotkov 1963)

burst was found to be sensitive to O_2 (Figure 2.16) and was closely related to photon irradiance during the preceding period of photosynthesis (Figure 2.17). Understandably, the Queens group regarded this post-illumination burst as a 'remnant' of respiratory processes in light, and coined the term 'photorespiration'. A functional link with the CO_2 compensation point was inferred, because the burst was also abolished in low O_2 (2% O_2 in Figure 2.16; see also Tregunna *et al.* 1966). Indeed, a competitive inhibition by O_2 on CO_2 assimilation was suspected and was subsequently proved to be particularly relevant in defining Rubisco's properties. Nevertheless, for many years a biochemical explanation for interaction between these two gases remained elusive.

Significant progress came when Ludwig and Krotkov (1967) designed an open gas exchange system in which $^{14}CO_2$ was used to separate the fixing (photosynthetic) and evolving (respiratory) fluxes of CO_2 for an illuminated leaf. Results using this steady-rate labelling technique were particularly revealing and provided the first direct evidence that respiratory process-

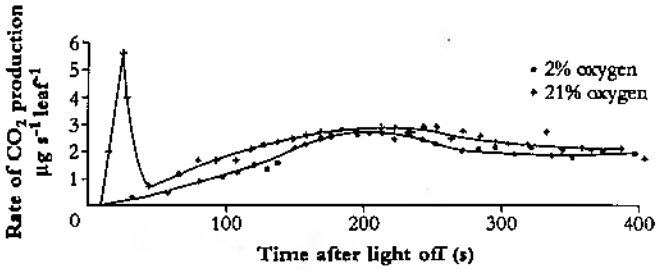

Figure 2.16 Photosynthesising leaves show a post-illumination burst of CO_2 which varies in strength according to surrounding O_2 concentration. This positive response to O_2 was observed at *c.* 105 μmol quanta $m^{-2}\ s^{-1}$ and is functionally linked to O_2 effects on the CO_2 compensation point (Figure 2.15) as measured under steady-state conditions
(Based on Krotkov 1963)

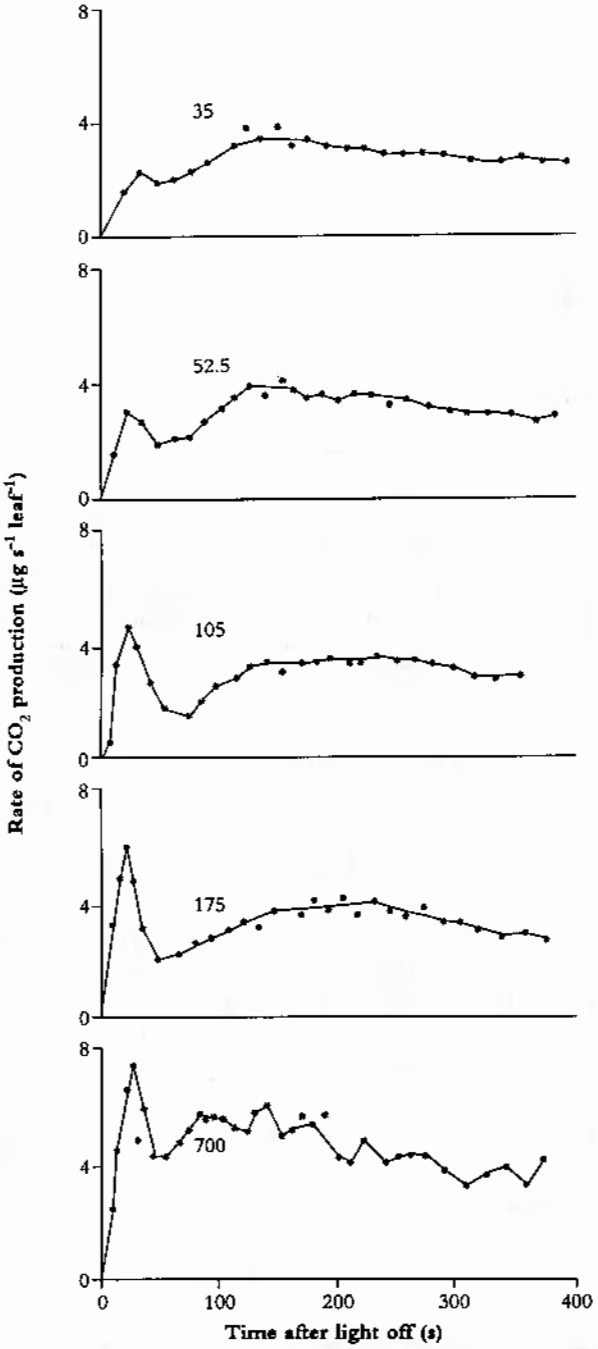

Figure 2.17 Photosynthesising leaves (in 21% O_2) show a post-illumination burst of CO_2 which varies in strength according to the intensity of preceding illumination shown here to range from 35 to 700 μmol quanta m^{-2} s^{-1} on each graph. (Original data in 'foot candles' have been converted to photon irradiance.) A large outburst occurred within the first minute with a second weaker emission of longer duration. Steady rates of CO_2 production were reached after *c.* 6 min
(Based on Krotkov 1963)

es in light were qualitatively different from those in darkness. In essence they were able to show that CO_2 evolved during normal high rates of photosynthesis by an attached sunflower leaf was derived from currently fixed carbon. Indeed the specific activity of evolved CO_2 (ratio of ^{14}C to ^{12}C) was essentially the same as that of the CO_2 being fixed, indicating that photorespiratory substrates were closely related to the initial products of fixation. Ludwig and Krotkov concluded that $^{14}CO_2$ supplied to a photosynthesising leaf was being re-evolved within 28–45 s! Furthermore the rate of CO_2 evolution in light was as much as three times the rate in darkness, and while early fixed products of photosynthesis (intermediates of the PCR cycle) were respired in light, this was not the case in darkness.

The radiolabelling method of Ludwig and Krotkov had, for the first time, provided measurements of what could be regarded as a true estimate of light-driven respiration which was not complicated by transient effects (as the post-illumination burst had been), or by changes in CO_2 concentration (as was the case for measurements in closed gas exchange systems or in CO_2-free air) or by difficulties associated with detached organs. Ludwig and Canvin (1971) subsequently concluded that processes underlying photorespiration re-evolved 25% of the CO_2 which was being fixed concurrently by photosynthesis. Clearly such a rate of CO_2 loss was not a trivial process so a biochemical basis for its operation had to be established, and particularly when photorespiration seemed to be quite different from known mechanisms of dark (mitochondrial) respiration.

2.3.2 Substrates for photorespiration

The search for the substrates of 'photorespiration' occupied many laboratories worldwide for many years. Much work centred on synthesis and oxidation of the two-carbon acid glycolate because as early as 1920 Warburg had reported that CO_2 fixation by illuminated *Chlorella* was inhibited by O_2, and under these conditions the alga excreted massive amounts of glycolic acid (Warburg and Krippahl 1960). Indeed numerous reports on the nature of the ^{14}C-labelled products of photosynthesis showed that glycolate was a prominent early-labelled product. A very wide variety of research with algae and leaves of many higher plants established two significant features of glycolate synthesis: formation was enhanced in either low CO_2 or high O_2. Both of these features had been predicted from Ludwig's (1968) physiological gas exchange work and eventually proved a key to understanding the biochemistry of photorespiration.

2.3.3 Localization of photorespiration

The PCR cycle for CO_2 fixation (Section 2.1) involves an initial carboxylation of ribulose-1,5-bisphosphate (RuBP) to form 3-PGA, but makes no provision for glycolate synthesis. However, Wang and Waygood (1962) and Tolbert (1963) had described the 'glycolate pathway', namely a series of reactions in which glycolate is oxidised to glyoxylate and aminated, first

to form glycine and subsequently the three-carbon amino acid serine. The intracellular location of this pathway in leaves was established in a series of elegant studies by Tolbert and his colleagues who also established that leaf microbodies (peroxisomes) were responsible for glycolate oxidation and the synthesis of glycine. Indeed Kisaki and Tolbert (1969) suggested that the yield of CO_2 from the condensation of two molecules of glycine to form serine could account for the CO_2 evolved in photorespiration. This idea was incorporated in later formulations of the pathway.

What remained elusive was the source of photosynthetically produced glycolate. Many studies had suggested that the sugar bisphosphates of the PCR cycle could yield a two-carbon fragment which, on the basis of short-term $^{14}CO_2$ fixation, would have its two-carbon atoms uniformly labelled (if the two-carbon were to be derived directly from 3-PGA this would not be the case as PGA was asymmetrically labelled in the carboxyl group). The mechanism was likened to the release of the active 'glycolaldehyde' transferred in the thiamine pyrophosphate (TPP)-linked transketolase-catalysed reactions of the PCR cycle. In some cases significant glycolate synthesis from the sugar bisphosphate intermediates of the cycle were demonstrated *in vitro;* however, the rates were typically too low to constitute a viable mechanism for glycolate synthesis *in vivo*.

A more dynamic approach to carbon fixation was needed to resolve this impasse. In particular, the biochemical fate of early products would have to be traced, and using a development of the open gas exchange system at Queens, Atkins *et al.* (1971) supplied $^{14}CO_2$ in pulse–chase experiments to sunflower leaf tissue under conditions in which photorespiration was operating at high rates (21% O_2) or in which it was absent (1% O_2). A series of kinetic experiments showed that synthesis of ^{14}C glycine and ^{14}C serine was inhibited in low O_2 and that the ^{14}C precursor for their synthesis was derived from sugar bisphosphates of the PCR cycle, especially RuBP. Indeed RuBP was the obvious source of glycine carbon atoms and the kinetics of glycine turnover closely matched those of RuBP. As these authors concluded, 'we can no longer view this (glycolate) pathway as an adjunct to the Calvin cycle but must incorporate it completely into the carbon fixation scheme for photosynthesis' (Atkins *et al.* 1971).

The question was finally and most elegantly resolved by Ogren and Bowes (1971) who demonstrated that the carboxylating enzyme of the PCR cycle, RuBP carboxylase, was *both* an oxygenase and a carboxylase! During normal photosynthesis in air, this enzyme thus catalysed formation of both P-glycolate (the precursor of glycolate) and 3-PGA from the oxygenation of RuBP as well as two molecules of PGA from carboxylation of RuBP. In effect, CO_2 and O_2 compete with each other for the same active sites for this oxygenation/carboxylation of RuBP, at last providing a biochemical mechanism which had confused and perplexed photosynthesis researchers since the 1920s. This primary carboxylating enzyme of the PCR cycle, which had hitherto rejoiced in a diversity of names (carboxydismutase, fraction 1 protein, RuDP carboxylase and RuBP carboxylase), was renamed Rubisco (ribulose-1,5-bisphosphate carboxylase/oxygenase) to reflect its dual activity.

A simplified scheme for the PCR cycle and photosynthetic carbon oxidation (PCO) pathways in Figure 2.18 represents the synthesis of almost 70 years research effort, and integrates the metabolism of P-glycolate with the PCR cycle. Specialised reactions within three classes of organelles in leaf cells are required, namely chloroplasts, microbodies and mitochondria. Their close proximity in leaf cells (Figure 2.11) plus specific membrane transporters (Secton 2.1.8) facilitate metabolite exchange. Oxygenase activity by Rubisco results in formation of phosphoglycolate (within chloroplasts) which then enters a PCO cycle, and is responsible for loss of some of the CO_2 just fixed in photosynthesis. During photorespiration, O_2 is consumed in converting glycolate to glyoxylate (within peroxisomes), while further CO_2 is released during subsequent condensation of glycine to serine (within mitochondria). Serine is recovered by peroxisomes where it is further metabolised, re-entering the PCR cycle of chloroplasts as glycerate. About 75% of carbon skeletons channelled into photorespiration are eventually recovered as carbohydrate.

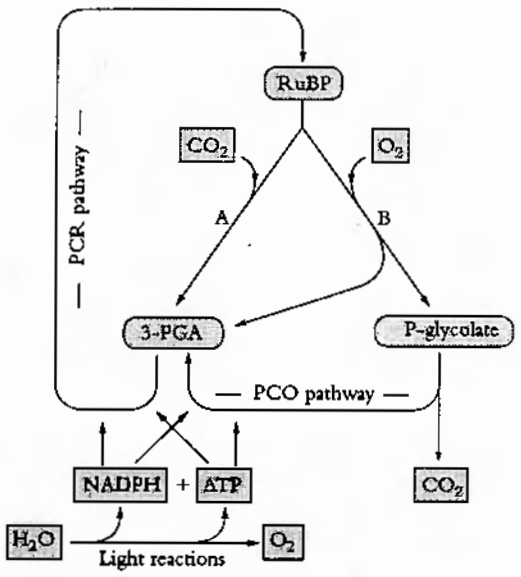

Figure 2.18 Photosynthetic carbon reduction (PCR) and photosynthetic carbon oxidation (PCO) pathways in green leaves are closely integrated. Rubisco in chloroplasts is initially responsible for both carboxylation and oxygenation of RuBP, and the balance between RuBP carboxylase (A) and RuBP oxygenase (B) reactions dictates the comparative rates of these two pathways. That poise in turn affects the net uptake of CO_2 per RuBP consumed and the energy input as ATP or NADPH, that is required for net uptake of CO_2. Energy (ATP) and reducing power (NADPH) derived from photosynthetic membranes are used to drive both cycles. Three ATP and two NADPH are consumed in regeneration of each RuBP via the PCR cycle; whereas 3.5 ATP and two NADPH are required for each oxygenation via the PCO pathway. One CO_2 is produced by photorespiration for every two oxygenations

(Based on Berry and Björkman 1980)

Participation of photorespiration in leaf gas exchange, and thus dry matter accumulation by plants, reflects kinetic properties of Rubisco, and in particular a relatively high affinity for CO_2 (K_m = 12 μM) compared with a much lower affinity for O_2 (K_m = 250 μM). That contrast in affinity is, however, somewhat offset by the relative abundance of the two gases at catalytic sites of the enzyme where the ratio of O_2:CO_2 partial pressures approaches 1000:1! Aided by an ordered reaction, CO_2 assimilation prevails, and a net fixation of carbon is an obvious outcome.

Not only does the photosynthetic oxidation pathway consume O_2 and release CO_2 but ammonia is also produced by mitochondria during synthesis of serine from glycine. This ammonia would be extremely toxic if it were not to be reassimilated by either cytosolic or chloroplastic glutamine synthetase. Indeed very effective herbicides which block glutamine synthetase have been developed (phosphinothricin or glufosinate) and when these are applied to actively growing plants they are killed by their photorespiratory ammonia release (herbicides are discussed further in Chapter 20).

2.3.4 C_4 plants and unicellular algae

At around the same time as the nature of photorespiration was becoming clearer Hatch and Slack (1966) demonstrated that in tropical grasses (initially sugar cane) the first-formed products of photosynthetic CO_2 fixation were the four-carbon acids oxalacetate, malate and aspartate, rather than the 3PGA formed in the PCR cycle. Furthermore, the carboxylation reaction involved PEP carboxylase and carbon was subsequently transferred to PCR cycle intermediates. As noted earlier (Sections 2.1, 2.2) C_4 plants show no apparent CO_2 release in light. The explanation lies in their anatomy and multiple carboxylation reactions rather than in the absence of the pathway of photorespiration. Bundle sheath cells are equipped with a CO_2-concentrating mechanism that favours carboxylation over oxygenation reactions due to increased partial pressure of CO_2, while photorespiratory release of CO_2 is further prevented through the activity of PEP carboxylase which refixes any respired CO_2 formed from the oxygenase function of Rubisco. Unicellular green algae also posed a problem for the simple extrapolation of early models for photorespiratory metabolism in C_3 leaves. Although organisms such as *Chlorella* had been used to establish the PCR cycle, and indeed provided much early evidence for effects of O_2 on photosynthesis and formation of glycolate in light, they also appeared to lack CO_2 evolution in light (Lloyd *et al.* 1977). In this case the explanation lies in a CO_2-concentrating mechanism which effectively increases the internal pool of inorganic carbon (CO_2 and HCO_3^-) thereby favouring the carboxylase function of Rubisco over its oxygenase function.

2.3.5 Does photorespiration represent lost productivity?

Such a substantial loss of carbon concurrent with CO_2 fixation raises the question of whether eliminating or minimising photorespiration in C_3 plants could enhance their yield, and specifically that of major crop plants such as rice, wheat, grain legumes, oil seeds and trees, all of which are not C_4 species. Faced with an expanding world human population and an increasing demand for food and animal feed, enhanced agricultural productivity is a global necessity. In its most obvious form a scenario which alters or removes the oxygenase function of Rubisco could achieve such a goal. However, in his review of the process of photorespiration in plants Ogren (1984) has noted that 'the sequence of reactions constituting the photorespiratory pathway in C_3 plants appears to be firmly established' and he goes on to suggest that, although reducing the loss of fixed carbon as CO_2 in the process may be a valid goal to improve the yield of crop plants, it is not clear whether or not this can be achieved by specific changes to the kinetic and catalytic properties of Rubisco alone.

Photorespiration may be loosely considered as a wasteful process because previously fixed carbon is lost and energy is dissipated. Ideal destinations for photoassimilates include synthetic pathways leading to fixed biomass and respiratory pathways for re-release of fixed energy in a controlled sequence of reactions leading to ATP and NAD(P)H for use in other synthetic events.

However, situations do exist where energy dissipation via photorespiration can be beneficial. For example, photo-oxidative damage can be alleviated in shade-adapted plants that experience strong irradiance if photorespiratory processes are allowed to proceed. Depriving such plants of an external oxygen supply, and hence preventing photosynthetic carbon oxidation, will exacerbate chloroplast lesions due to strong irradiance. Photosynthetic variants which obviate photorespiratory loss and most notably C_4 plants integrate structure and function in a way that forestalls photo-oxidative damage and leads to their outstanding performance nnder warm conditions. Environmental factors that constitute selection pressure for such photosynthetic adaptation and the general ecology of photosynthesis in sun and shade are discussed further in Chapter 12.

2.4 Respiration and energy generation

During respiration, the product pair from photosynthesis (O_2 and reduced carbon) are reunited to yield energy. Cellular metabolites are oxidised as electrons are transferred through a series of electron carriers to O_2. Water and CO_2 are formed

and energy is captured as ATP and other forms suitable for metabolic work. Sucrose and starch are prime sources of respiratory substrates in plants, although other carbohydrates such as fructans and sugar alcohols are also utilised. In comparison to sucrose and starch, the contribution of proteins and lipids as sources of respiratory substrates in most plant tissnes is minor; exceptions to this generalisation are the storage tissues of seeds such as castor bean and soybean, in which amino acids and lipids may provide respiratory substrates.

2.4.1 Starch and sucrose degradation

Starch is the major carbon reserve in most plants. It is a mixture of amylose and amylopectin and is deposited as granules inside plastids (chloroplasts in leaves, amyloplasts in non-photosynthetic tissues). The initial attack on starch granules in leaves and non-photosynthetic tissues is by α-amylase and a debranching enzyme. Oligosaccharides released during starch degradation, such as maltose, maltotriose and maltotetraose, are hydrolysed to glucose by α-glucosidase. These processes are summarised in Figure 2.19.

Reactions in plant tissues leading to degradation of sucrose to hexose monophosphates are outlined in Figure 2.20. The first step is cleavage of the glycosidic bond by either invertase (Equation 2.1) or sucrose synthase (Equation 2.2).

$$\text{Sucrose} + H_2O \rightarrow \text{D-glucose} + \text{D-fructose} \quad (2.1)$$

$$\text{Sucrose} + \text{UDP} \rightarrow \text{UDP-glucose} + \text{D-fructose} \quad (2.2)$$

Plant tissues contain two types of invertases which hydrolyse sucrose to glucose and fructose in an essentially irreversible reaction: acid invertase, which has optimum activity near pH 5, and is present in vacuoles, the free space outside cells, and may be associated with the cell wall; and alkaline or neutral invertase, which is maximally active at about pH 7 to 7.5 and is located in the cytosol. Sucrose synthase is a cytosolic enzyme that catalyses a readily reversible reaction, but probably acts only in the breakdown of sucrose *in vivo*. Sucrose appears to be partitioned between alkaline invertase and sucrose synthase in the cytosol on the basis of differences in affinity of the two enzymes for the substrate. (K_m values for sucrose of alkaline invertase and sucrose synthase generally fall within the ranges 10–15 mM and 20–30 mM, respectively.) Glucose and fructose are metabolised further following phosphorylation to the corresponding hexose-6-P, probably by separate enzymes for the two hexoses. Plant tissues contain several hexose kinases that have specificity towards either glucose or fructose. A substantial portion of the glucose kinase in plant tissues is associated with the outer surface of the outer mitochondrial membrane, while fructokinases appear to be soluble in the cytosol.

Two molecules of ATP are required to metabolise the hexoses formed upon cleavage of sucrose by invertase. However, when sucrose is cleaved by sucrose synthase, part of the energy in the glycosidic bond is conserved in the UDP-glucose formed and only one molecule of ATP is required for the further metabolism of fructose. UDP-glucose may be converted to glucose-1-P by UDP-glucose pyrophosphorylase. Glucose-1-P is converted to glucose-6-P, and glucose-6-P to fructose-6-P, by phosphoglucomutase and phosphohexose isomerase, respectively.

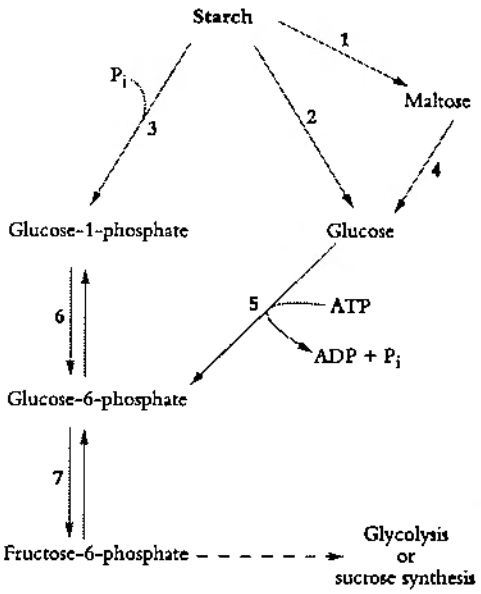

Figure 2.19 Pathways of starch metabolism. Numbers refer to the following enzymes. 1, β-amylase; 2, α-amylase; 3, starch phosphorylase; 4, glucosidase; 5, hexose kinase; 6, phosphoglucomutase; 7, glucose 6-phosphate isomerase
(Original drawing courtesy David Day)

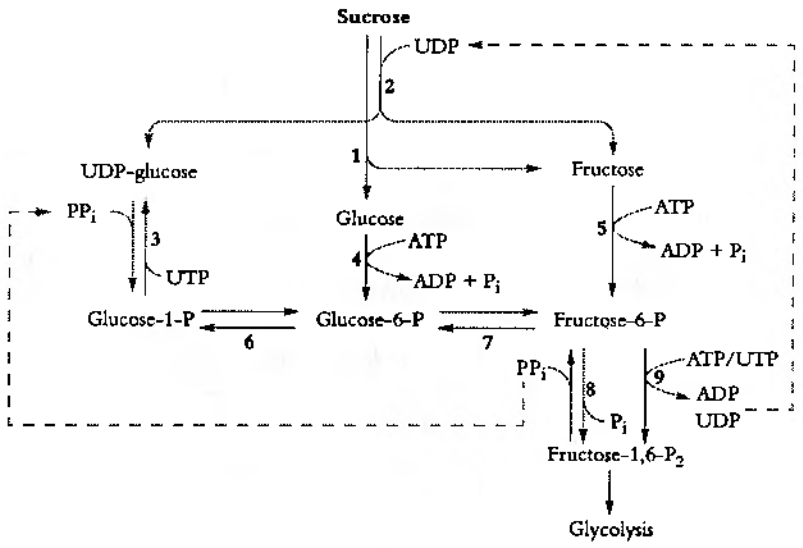

Figure 2.20 A scheme for breakdown of sucrose in plants. Broken lines indicate possible interconnecting reactions. Numbers refer to the following enzymes: 1, invertase; 2, sucrose synthase; 3, UDP-glucose pyrophosphorylase; 4, hexokinase; 5, fructokinase; 6, phosphoglucomutase; 7, phosphohexose isomerase; 8, phosphofructophosphotransferase; 9, phosphofructokinase
(Original drawing courtesy David Day)

2.4.2 The glycolytic pathway

Glycolysis originally described the sequence of reactions that convert glycogen to lactic acid in muscle and is usually considered to include the metabolism of hexose phosphates to pyruvate. In plant tissues, starch takes the place of glycogen in this scheme, and there is probably a second end-product, either oxaloacetate or malate (Figure 2.21).

Moreover, in plants glycolysis occurs in both cytosol and plastids, with reactions in the different compartments catalysed by separate isoenzymes. The first step in the pathway is phosphorylation of fructose-6-P to fructose-1,6-P_2. Plant tissues contain two enzymes capable of catalysing this step: an ATP-dependent phosphofructokinase (PFK), which catalyses an essentially irreversible reaction and occurs in the cytosol and plastids, and phosphofructophosphotransferase (PFP) (now called PP_i-dependent phosphofructokinase, PP_i-PFK), which occurs only in the cytosol and utilises PP_i as the phosphoryl donor in a reaction that is readily reversible.

Regulation of PFK is achieved by a combination of mechanisms, including pH, the concentration of substrates and effector metabolites, changes in the state of aggregation, and covalent modification by phosphorylation/dephosphorylation of the protein. The relative importance of these mechanisms varies depending on the organism. In plants phosphoenolpyruvate (PEP) is probably the most potent regulator, inhibiting at mM concentrations, but 3-PGA and 2-PGA also strongly inhibit. P_i activates the cytoplasmic PFK, and to a lesser extent that from plastids, and overcomes the inhibition by PEP. The enzyme is also activated by Cl^- and other anions. The regulatory metabolite fructose-2,6-P_2, a powerful activator of PFK from animals, has no effect on the enzyme from plants.

PFP, discovered subsequently, is ubiquitous in plants and has a catalytic potential higher than that of PFK. Fructose-2,6-P_2 strongly activates PFP, but the physiological significance of this activation and, indeed, the role of PFP, in plants have not yet been clearly established. Fructose-2,6-P_2 is a potent inhibitor of cytosolic fructose-1,6-bisphosphatase which is an important control point of sucrose biosynthesis regulating the partitioning of photosynthate between sucrose and starch in leaves. Whether fructose-2,6,-P_2 has a role in the control of glycolysis through its activation of PFP is not clear.

Since the reaction catalysed by PFP is reversible and the concentration of fructose-2,6-P_2 in the cytosol is usually high enough to maintain PFP in an activated form, the direction of this reaction *in vivo* is likely to depend on availability of substrates. In tissues where sucrose breakdown is occurring, PFP may function to generate PP_i to facilitate the conversion of UDP-glucose to glucose-1-P (Figure 2.20). Under these conditions, the simultaneous and opposing action of PFK and PFP in the cytosol could set up a potentially wasteful substrate cycle between fructose-6-P and fructose-1,6-P_2. The operation of such a cycle may be a cost of having a mechanism to generate PP_i and, ultimately, UDP for the breakdown of sucrose by sucrose synthase. PFP may also act as an inducible enzyme in some plant tissues, providing increased glycolytic capacity when required during certain stages of plant development, or during adjustment to adverse environmental conditions.

Fructose-1,6-P_2 is cleaved by aldolase to form dihydroxyacetone-P and glyceraldehyde 3-P, and these triose phosphates are interconverted in a reaction catalysed by triose phosphate isomerase. Glyceraldehyde 3-P is oxidised to glycerate-1,3-P_2 by an NAD-dependent glyceraldehyde 3-P dehydrogenase in the cytosol and an NADP-linked enzyme in plastids. Glyceraldehyde 3-P dehydrogenase is sensitive to inhibition by the reduced pyridine nucleotide cofactor, which must be reoxidised to maintain the flux through the glycolytic pathway. In chloroplasts, the reactions catalysed by fructose-1,6-P_2 aldolase, triose phosphate isomerase and NADP-dependent glyceraldehyde 3-P dehydrogenase also form part of the PCR cycle. The remaining steps for PEP formation are shown in Figure 2.21; all steps from fructose-1,6-P_2 to PEP are reversible.

The end-product of glycolytic reactions in the cytosol of plants is determined by the relative activities of the two enzymes that can utilise PEP as a substrate: pyruvate kinase, which forms pyruvate and a molecule of ATP, and PEP carboxylase, which forms oxaloacetate (Figure 2.21). Both of these reactions are essentially irreversible and there are fine controls that regulate the partitioning of PEP between these reactions. Pyruvate kinase requires monovalent cations and is inhibited by ATP (and therefore is sensitive to the energy status of the cell), whereas PEP carboxylase is inhibited by malate and is independent of cell energy status. The sensitivity of PEP carboxylase to malate is regulated by phosphorylation of the enzyme by a protein kinase: the phosphorylated form is less sensitive to malate inhibition. This phosphorylation may form part of an important diurnal regulatory cycle in the leaves of crassulacean acid metabolism plants (see Section 2.1).

Oxaloacetate is reduced by malate dehydrogenase to malate which, along with pyruvate, can be taken up into mitochondria and metabolised further (see below). The reduction of oxaloacetate in the cytosol could provide a cytosolic mechanism for oxidising NADH formed by glyceraldehyde 3-P dehydrogenase (Figure 2.21).

In chloroplasts glycolysis is most active in conjunction with the breakdown of starch to form sucrose for export to non-photosynthetic tissues. There is some doubt about the occurrence of phosphoglycerate mutase in chloroplasts, and therefore the main products of the glycolytic reactions may be triose phosphates and 3-PGA. These could be exported through the P_i translocator in the chloroplast envelope to the cytosol, where sucrose synthesis takes place. In photosynthetic cells, the triose P exported to the cytosol for sucrose synthesis (Section 2.1.8) could also enter the glycolytic pathway directly to provide mitochondrial substrates.

Studies of changes in the content of glycolytic intermediates in plant tissues that undergo an altered rate of

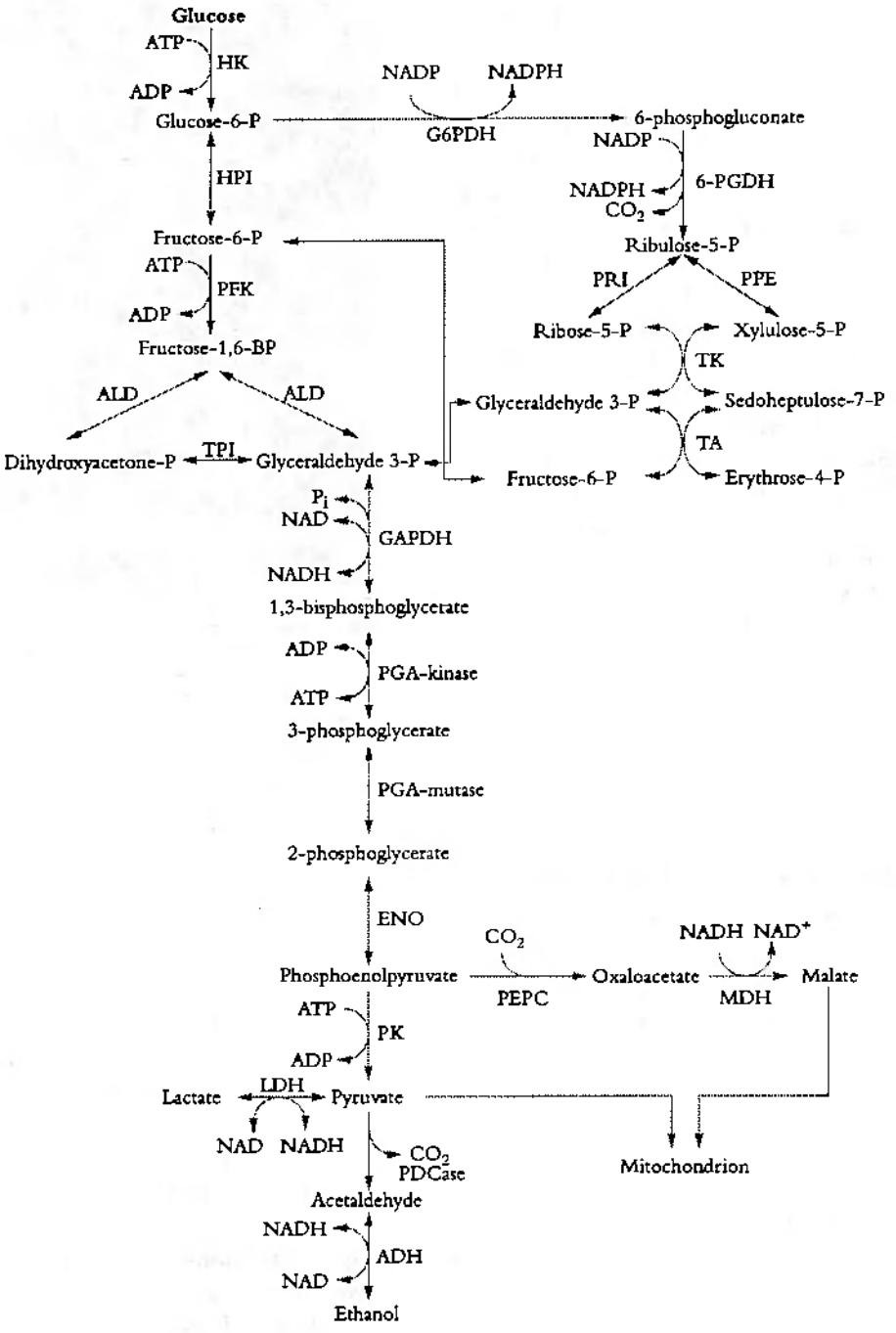

Figure 2.21 Interrelationships between glycolysis and the pentose phosphate pathway. Enzymes abbreviated are: HK, hexokinase; HPI, hexose phosphate isomerase; PFK, phosphofructokinase; ALD, aldolase; TPI, triose phosphate isomerase; GAPDH, glyceraldehyde 3-phosphate dehydrogenase; PGA, phosphoglycerate; ENO, enolase; PK, pyruvate kinase; PDC, pyruvate decarboxylase; ADH, alcohol dehydrogenase; LDH, lactate dehydrogenase, G6PDH, glucose-6-phosphate dehydrogenase; 6-PGDH, 6-phosphogluconate dehydrogenase; PRI, phosphoriboisomerase; PPE, pentose phosphate epimerase; TK, transketolase; TA, transaldolase; PEPC, phosphoenolpyruvate carboxylase; MDH, malate dehydrogenase. Note that lactate and ethanol are formed only when mitochondrial function is inhibited, as under anaerobiosis
(Original drawing courtesy David Day)

respiration (e.g. during the climacteric in ripening fruits or in plant tissues placed under low-O_2 stress) indicate that the conversion of fructose-6-P to fructose-1,6-P_2, and PEP to pyruvate, are major regulatory steps. For example, a decrease in activity of PEP carboxylase and pyruvate kinase (the latter in response to a lower energy demand as indicated by an increase in the cytosolic ATP/ADP ratio) can lead to an increase in the concentration of inhibitory metabolites of PFK and, consequently, a decrease in the rate of glycolysis. The rate of oxidation of NAD(P)H is also likely to have a bearing on the glycolytic flux at the glyceraldehyde 3-P dehydrogenase step.

2.4.3 Pentose phosphate pathway

An alternative route for the breakdown of glucose-6-P is provided by the pentose phosphate pathway (Figure 2.21, right side). This pathway functions mainly to generate NADPH and precursors for various biosynthetic processes. These include ribose-5-P, which provides the ribosyl moiety of nucleotides and is a precursor for the biosynthesis of the purine skeleton, and erythrose-4-P, for the biosynthesis of aromatic compounds in the shikimic acid pathway. Glyceraldehyde 3-P and fructose-6-P formed in the pentose phosphate pathway may be metabolised further in the glycolytic pathway. Alternatively, fructose-6-P may be converted back to glucose-6-P by phosphohexose isomerase and recycled through the pentose phosphate pathway. The pentose phosphate pathway may account for between 15 and 30% of the hexose phosphate oxidised to glyceraldehyde 3-P and CO_2.

As with glycolysis, reactions of the pentose phosphate pathway are catalysed by different sets of isoenzymes that occur either in the cytosol or in plastids. The reactions in the non-oxidative phase of the pentose phosphate pathway are readily reversible and also form part of the PCR cycle of chloroplasts.

2.4.4 Mitochondria and organic acid oxidation

Organic acids produced in the cytosol by processes described above are further oxidised in mitochondria via the tricarboxylic acid (TCA) or Kreb's cycle and subsequent respiratory chain. Energy released by this oxidation is used to synthesise ATP which is then exported to the cytosol for use in biosynthetic events.

(a) Mitochondrial structure

Plant mitochondria (Figure 2.22) are typically double-membrane organelles where the inner membrane is invaginated to form folds ('cristae'). The outer membrane contains relatively few proteins and is permeable to most compounds of less than 5 kDa molecular weight, by virtue of a pore-forming protein ('porin'). This outer membrane also contains an NADH dehydrogenase and a *b*-type cytochrome whose function is not understood. The inner membrane is the main permeability barrier of the organelle and controls the movement of molecules by means of a series of carrier proteins. The inner membrane also houses the redox carriers of the respiratory chain and delineates the soluble matrix which contains the enzymes of the TCA cycle, other soluble proteins and the protein synthesising machinery.

Mitochondria are semi-autonomous organelles with their own DNA and protein synthesising machinery. However, the mitochondrial genome codes for only a small portion of the proteins which make up the mitochondrion; the rest are encoded on nuclear genes and synthesised in the cytosol. These proteins are transported into the mitochondrion and assembled with the mitochondrially synthesised proteins to form respiratory complexes. The number of mitochondria per cell varies with tissue type (from a few hundred in mature differentiated tissue to some thousands in specialised cells such as those in the infected zone of N_2-fixing nodules; Millar *et al.* 1995b). Understandably, more active cells such as those in meristems are generally equipped with larger numbers and consequently show faster respiration rates.

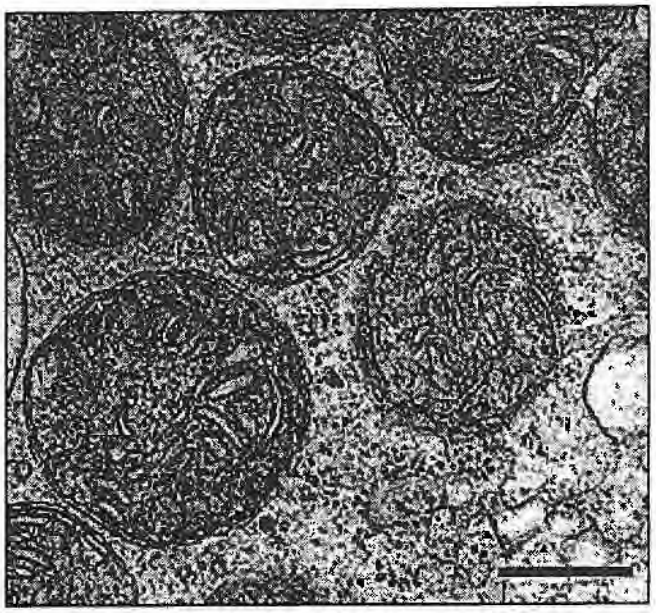

Figure 2.22 Transmission electron micrograph of a parenchyma cell in a floral nectary of broad bean (*Vicia faba*) showing an abundance of mitochondria, generally circular in profile and varying between about 0.75 and 1.5 μm in diameter. Each mitochondrion is encapsulated by an outer and inner membrane which is in turn infolded to form cristae. Under higher magnification, 'knobs' are seen to protrude from this inner membrane and are now recognised as ATP synthase complexes (refer to Figure 1 in Case study 2.1). Cytoplasmic ribosomes are also apparent, many of which have been organised into polyribosomal helices. Horizontal bar (bottom right) is 0.5 μm
(Original electron micrograph courtesy Brian Gunning)

(b) Mitochondrial substrates

Two substrates are produced from glycolytic PEP for oxidation in mitochondria: malate and pyruvate (Figure 2.21). These compounds are thought to be the most abundant mitochondrial substrates *in vivo*. However, amino acids may also serve as substrates for mitochondrial respiration in some tissues, particularly in seeds rich in stored protein. This oxidation may be preceded by transamination within the mitochondrion to produce a TCA cycle intermediate, or in some cases may occur directly. For example, most mitochondria contain glutamate dehydrogenase which oxidises glutamate to α-ketoglutarate and produces NADH (as well as ammonia). Some mitochondria also contain proline and glycine dehydrogenases, enzymes that feature in photorespiration and are largely confined to leaf mitochondria (Section 2.3). β-oxidation of fatty acids can occur in plant mitochondria, although this oxidation is slow compared to that in animal mitochondria (most fatty acid oxidation in plants occurs in microbodies).

(c) Carbon metabolism in mitochondria

Malate and pyruvate enter the mitochondrial matrix across the inner membrane via separate carriers. Malate is then oxidised by two enzymes: malate dehydrogenase (a separate isoenzyme from that in the cytosol), which yields OAA and NADH, and NAD-linked malic enzyme, which yields pyruvate and NADH and releases CO_2 (Figure 2.23).

Pyruvate formed either from malate or transported directly from the cytosol is oxidised by the key enzyme pyruvate dehydrogenase to form CO_2, acetyl-CoA and NADH. This enzyme, which requires coenzyme A, thiamine pyrophosphate and lipoic acid as cofactors, effectively links the TCA cycle to glycolysis. It consists of a complex of three enzymes: pyruvate dehydrogenase itself, dihydrolipoyl transacetylase and the flavoprotein dihydrolipoyl dehydrogenase. The pyruvate dehydrogenase complex has a molecular weight in the millions and is subject to sophisticated regulatory mechanisms, including phosphorylation/dephosphorylation by a kinase/phosphatase couple. Reversible phosphorylation by the kinase inactivates the enzyme and various factors regulate the kinase (e.g. pyruvate inhibits it whereas ammonia stimulates it). Pyruvate dehydrogenase is also subject to feedback inhibition from acetyl-CoA and NADH.

(d) Tricarboxylic acid (TCA) cycle

The TCA cycle proper begins with a condensation of acetyl-CoA and OAA, to form the six-carbon molecule citrate and release CoA (Figure 2.23) (a reaction catalysed by citrate synthase). Aconitase catalyses the next step, converting citrate to isocitrate. Both of these enzymes occur as isoenzymes in other cellular compartments, citrate synthase in glyoxisomes of oil seeds and aconitase in the cytosol.

NAD-linked isocitrate dehydrogenase then oxidatively decarboxylates isocitrate to form CO_2 and α-ketoglutarate, and reduce NAD^+. The α-ketoglutarate thus formed is oxidised further to succinyl-CoA in a reaction catalysed by the enzyme α-ketoglutarate dehydrogenase. This enzyme is a complex that has similarities to pyruvate dehydrogenase and the reaction is analogous to the formation of acetyl-CoA from pyruvate. The reaction mechanisms are also very similar but α-ketoglutarate dehydrogenase is not subject to the complicated control of pyruvate dehydrogenase. Succinyl-CoA synthase then catalyses the conversion of succinyl-CoA to succinate, with the concomitant phosphorylation of ADP to ATP, the only substrate-level phosphorylation step in the mitochondrion. This enzyme in plants differs from its mammalian counterpart in that it is specific for ADP rather than GDP.

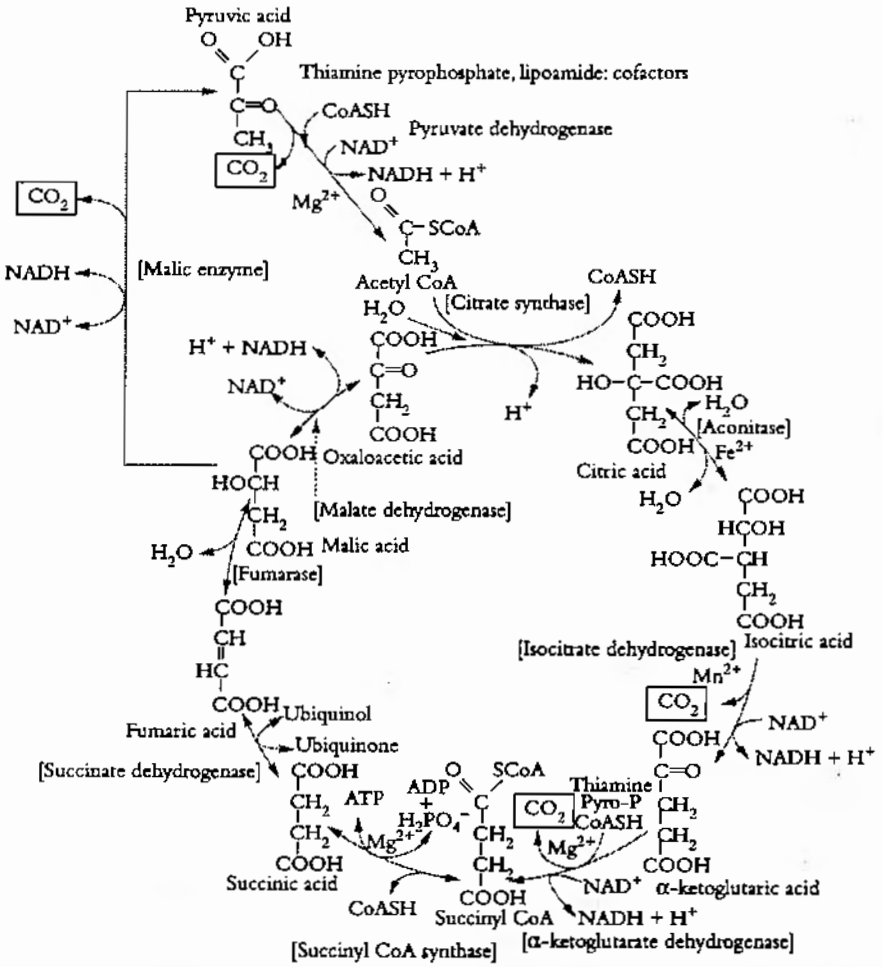

Figure 2.23 Tricarboxylic acid cycle with appendages. Glycolysis in the cytoplasm yields pyruvate or malate as substrates. Malic enzyme catalyses the decarboxylation of malate to pyruvate within the mitochondria (Original drawing courtesy David Day)

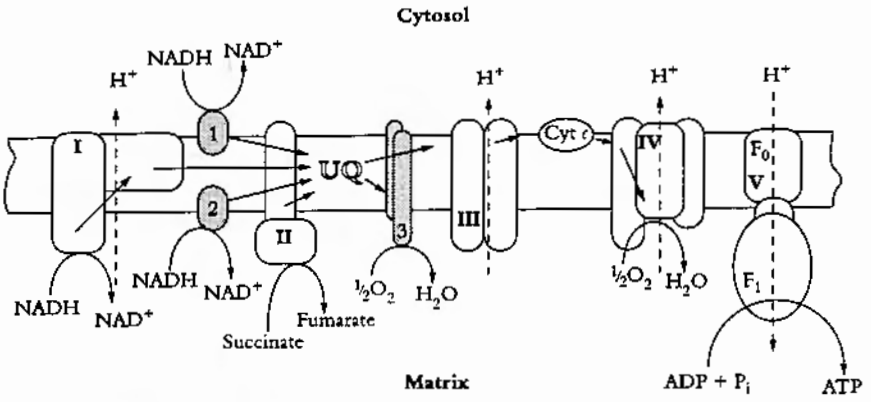

Figure 2.24 Electron transport chain of plant mitochondria. Roman numerals indicate respiratory complexes equivalent to mammalian counterparts. Complex I, NADH-UQ oxido-reductase; complex II, succinate dehydrogenase; complex III, Cyt b/c_1 complex; complex IV, Cyt *c* oxidase; complex V, ATP synthetase. Arabic numerals indicate special plant features: 1, external NADPH dehydrogenase; 2, internal, rotenone-insensitive NADH dehydrogenase; 3, alternative (cyanide-insensitive) oxidase; UQ, ubiquinone. Unbroken arrows indicate pathways of electron flow; broken arrows indicate proton translocation sites
(Original drawing courtesy David Day)

Succinate dehydrogenase (SDH), which catalyses the oxidation of succinate to fumarate, is the only membrane-bound enzyme of the TCA cycle and is part of the respiratory electron transport chain (complex II, Figure 2.24). SDH is a complex consisting of a flavoprotein and several other subunits; the former has FAD as a covalently bound cofactor and the enzyme also contains two bi-nuclear iron–sulphur clusters. Electrons from $FADH_2$ are passed on to ubiquinone.

Fumarase catalyses the conversion of fumarate to malate and is unique to the mitochondrion, making it a convenient marker for the mitochondrial matrix. Malate dehydrogenase catalyses the final step of the TCA cycle, oxidising malate to OAA and producing NADH. The reaction is freely reversible, although the equilibrium constant strongly favours the reduction of OAA, necessitating rapid turnover of OAA and NADH to maintain this reaction in a forward direction.

Overall, during one turn of the cycle, three carbons of pyruvate are released as CO_2, one molecule of ATP is formed directly, and four NADH and one $FADH_2$ are produced. The latter strong reductants are oxidised in the respiratory chain to reduce O_2 and produce ATP. Although most of the TCA cycle enzymes in plant mitochondria are NAD linked, NADP-dependent isoforms of isocitrate and malate dehydrogenases also exist, and these may play a role in a protective reductive cycle in the matrix.

Regulation of carbon flux through the TCA cycle probably occurs via phosphorylation/dephosphorylation of pyruvate dehydrogenase, which will depend in turn on mitochondrial energy status and feedback inhibition of various enzymes by NADH and acetyl-CoA. The rate of cycle turnover thus depends on the rate of electron flow through the respiratory chain (to reoxidise NADH) and utilisation of ATP. TCA cycle turnover will also depend on the rate of substrate provision by reactions in chloroplasts and cytosol, and in pea leaves this may be a major limitation on the rate of respiration *in vivo*. For example, in an experiment to estimate respiratory chain capacity, Wiskich and Dry (1985) isolated mitochondria from pea leaves and resuspended them in a known volume of reaction medium. A large proportion of organelles is usually ruptured during isolation, and it is important to estimate yield of intact mitochondria. Therefore the volume of the leaf homogenate obtained upon disruption of the leaves was also measured, and a small aliquot set aside. A mitochondrial marker for enzyme activity (e.g. fumarase) was measured for both isolated mitochondria preparation and crude homogenate. The percentage yield of intact mitochondria was inferred from their comparative activities. Respiration rate by isolated mitochondria was then measured in an oxygen electrode with a mixture of substrates. That value was extrapolated to a mitochondrial capacity of a whole leaf by correcting for the yield of intact mitochondria. In a parallel experiment, the *in vivo* rate of respiration by intact leaf tissue was measured in a second oxygen electrode. Comparative values were as follows:

Rate of respiration by mitochondrial suspension: 220 μmol O_2 h^{-1}
Per cent yield of mitochondria: 50
Fresh mass of leaf tissue: 10 g
Respiratory capacity of tissue: 44 μmol O_2 h^{-1} g^{-1}
Respiratory rate of intact leaf tissue: 23 μmol O_2 h^{-1} g^{-1}

Respiratory capacity as inferred from the activity of isolated mitochondria exceeded actual measured rates of intact leaf tissue. Respiration *in vivo* is therefore constrained, and such restriction might be due to either substrate supply and/or ATP/ADP ratio.

2.4.5 Respiratory chain

The respiratory chain of mitochondria consists of a series of membrane-bound redox centres which catalyse the transfer of electrons from NADH and $FADH_2$ to O_2, forming water and

translocating protons across the inner membrane (Figure 2.24). Translocation of protons is made possible by release of redox energy that accompanies electron transfer from the strong reductant NADH to the strong oxidant O_2, and is functionally linked to electron transfer. (This electron transfer involves a release in redox energy of 1.14 V which is equivalent to 52.7 kcal of chemical energy, enough to drive the synthesis of three ATP molecules.) In this way, a protonmotive force ($\Delta\mu_H{}^+$) is created across the inner membrane and is used to drive phosphorylation of ADP via the ATP synthase complex (Figure 2.24 right side).

Plant mitochondria have a respiratory chain which is more complicated than that of animals and contains additional NADH dehydrogenases and an alternative oxidase which catalyses cyanide-insensitive O_2 consumption. These additional enzymes (which are also found in most fungi) do not translocate protons and therefore are not linked to ATP synthesis; they are often referred to as the non-phosphorylating bypasses of the plant respiratory chain. The other complexes of the chain are common to all mitochondria and have been extensively studied in animals and fungi and to some extent in plants. They have been assigned roman numerals by researchers of mammalian respiration (Figure 2.24).

According to structural arrangements that underlie electron transport in plant mitochondria, large protein-containing complexes of the respiratory chain are immersed in the inner membrane by virtue of their hydrophobic subunits, and interact with one another via two smaller molecules: ubiquinone and cytochrome *c*. The lipid-soluble ubiquinone is small enough to move rapidly along and across the membrane, and participates in H^+ transport across the membrane as well as shuttling electrons from complexes I and II to complex III. Location and oxidation–reduction status are shown in Figure 2.25. Cytochrome *c* is a small haem-containing protein located on the outer surface of the inner membrane, which shuttles electrons between complexes III and IV. In this respect, the respiratory chain is similar in layout to the photosynthetic electron transport chain: three large complexes which communicate by a quinone and a small mobile protein (Cyt *c* or plastocyanin). However, orientation of components in the membrane is inverted and the net reaction catalysed is opposite to that in chloroplasts (Figure 2.13).

(a) NADH oxidation

Complex I, NADH-ubiquinone oxido-reductase (Figure 2.24), is a large multi-subunit complex of 30–40 polypeptides, seven of which are synthesised in the mitochondrion. One of the subunits, a 50 kDa protein, contains flavinmononucleotide as a cofactor and is the dehydrogenase which oxidises NADH and passes electrons to FeS-containing proteins of the complex, and eventually to ubiquinone. The passage of electrons through the complex is accompanied by H^+ translocation across the membrane (mechanism poorly understood). Complex I is inhibited specifically by the flavonoid rotenone and analogues. The NADH-binding site is exposed to the matrix and the complex oxidises NADH produced by TCA cycle and other NAD-linked enzymes.

Plant mitochondria contain another matrix-located NADH dehydrogenase which is insensitive to rotenone and does not pump protons across the membrane (called the 'rotenone-insensitive bypass'). Plant mitochondria also oxidise NADH and NADPH by two dehydrogenases on the outside of the inner membrane. This oxidation is not inhibited by rotenone and is not linked to H^+ translocation. These external dehydrogenases are presumed to oxidise NAD(P)H produced in the cytosol.

(b) Succinate oxidation

Complex II (Figure 2.24) is succinate dehydrogenase, which also spans the membrane and has its active site exposed to the matrix. It consists of five subunits, one of which is encoded by the mitochondrial genome in plants while the rest are synthesised in the cytosol. SDH also contains FeS and haem centres which participate in electron transfer from succinate to ubiquinone. Unlike complex I, complex II does not pump H^+ and succinate oxidation is therefore linked to the synthesis of less ATP (see below). Malonate, an analogue of succinate, is a strong competitive inhibitor of succinate dehydrogenase.

(c) Cytochromes

Complex III (Figure 2.24) is the cytochrome b/c_1 complex, consisting of two *b*-type cytochromes, b_{566} and b_{562}, cytochrome c_1, an FeS protein named the Rieske iron–sulphur protein and several other polypeptides. The complex contains eight subunits, one of which is synthesised in the mitochondrion. Electron flow from ubiquinol to cytochrome *c* is accompanied by the translocation of four H^+ per electron pair, across the membrane, via the so-called Q cycle. According to this mechanism, ubiquinone is reduced on the matrix side of the membrane by one electron from complex I or II and one from Cyt b_{562}. The quinol then diffuses across to the outside of the membrane to reduce Cyt c_1 and the Rieske FeS centre; the electron from c_1 is passed on to *c* and then in turn to cytochrome oxidase, while the FeS electron is handed on to Cyt b_{566}, then to b_{562}, which reduces ubiquinone. Thus the *b* cytochromes participate in the movement of electrons across the complex but do not participate in the reduction of Cyt *c* (Figure 2.25). Various inhibitors of complex III have been discovered, with antimycin A and myxothiazol most widely used in research.

The final complex of the main respiratory chain (Figure 2.24) is complex IV, cytochrome *c* oxidase. As the name implies, cytochrome *c* oxidase accepts electrons from cytochrome *c* on the outside of the inner membrane and transfers them to the inside of the membrane where O_2 is reduced to form H_2O. The complex contains 7–9 polypeptides (three of which are synthesised in the mitochondrion). Two cytochrome haem centres, *a* and a_3, and two copper atoms make up its redox active components. Like complex I, cytochrome oxidase is a proton pump, but the mechanism is still poorly defined.

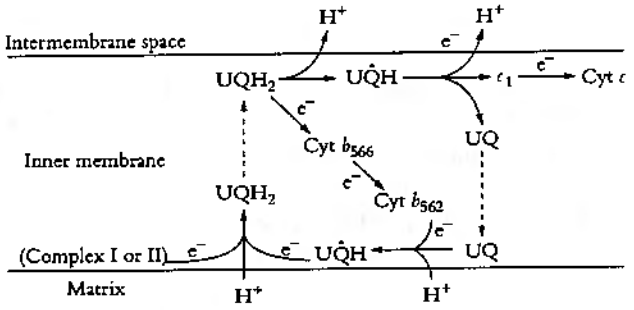

Figure 2.25 The protonmotive Q cycle mechanism of proton translocation at complex III of the respiratory chain. Oxidised quinone (UQ) accepts an electron from Cyt b_{562} of complex III and a proton from the matrix to form the semiquinone (UQH). The semiquinone accepts another proton from the matrix and an electron from complex I (or II) to form the quinol which then diffuses across the membrane (broken arrows) to interact with Cyt b_{566} and the FeS protein of complex III near the outside of the inner membrane. UQH2 is oxidised to the semiquinone by Cyt b_{566}, losing a proton to the external medium in the process, which then reduces b_{562}. The semiquinone is oxidised by the FeS protein (not shown), losing another proton which then reduces Cyt c_1 and thence Cyt c. The quinone formed then diffuses back across the membrane to interact with Cyt b_{562}. In this way, one electron is transferred from complex I (or II) on one side of the membrane, to Cyt c on the other, with another electron and UQ shuttling back and forth across the membrane. Concurrently, two H^+ are translocated from the matrix to the external medium for each electron flowing to Cyt c. Broken arrows indicate diffusion of both fully oridised and fully reduced ubiquinone; unbroken arrows indicate electron flow
(Original drawing courtesy David Day)

2.4.6 Oxidative phosphorylation

When electrons are transferred from NADH to O_2, a large release of redox energy enables ATP formation in complex V of the respiratory chain (ATP synthase in Figure 2.24). Energy release associated with electron transport is conserved by H^+ translocation across the membrane to form a protonmotive force ($\Delta\mu_H{}^+$) which has both an electrical and a pH component ($\Delta\mu_H{}^+ = \Delta\psi + \Delta pH$). This forms the basis of the chemiosmotic theory proposed by Mitchell in 1960 and now widely accepted.

In plant mitochondria, ($\Delta\mu_H{}^+$) exists mainly as a Dy of 150–200 mV, with a pH gradient (ΔpH) of 0.2–0.5 units. ATP synthesis occurs as H^+ move from a compartment of high potential (outside the membrane) to one of low potential (the mitochondrial matrix) through the ATP synthase complex. Oxidation of NADH via the cytochrome pathway has three H^+ translocation sites associated with this process, and is linked to synthesis of up to three ATP molecules for each molecule of NADH oxidised (i.e. three ATP formed per two electrons). By contrast, both succinate and external NADH oxidation, or NADH oxidation via the rotenone-insensitive bypass, are linked to the synthesis of only two ATP molecules per two electrons, as these events are associated with only two H^+ pumping sites.

The number of H^+ translocated for each pair of electrons transferred from NADH to O_2 remains controversial; it will depend, in the final analysis, on the mechanism(s) by which H^+ translocation is coupled to electron flow and this has still to be elucidated. Given the magnitude of free energy change during ATP synthesis and the magnitude of measured $\Delta\mu_H{}^+$, at least three H^+ are needed per ATP synthesised. Consequently, the $H^+/2e^-$ ratio for oxidation of NADH must be at least 9.

(a) ATP synthase

ATP synthase is another multi-subunit complex (Figure 2.26) with at least nine polypeptides, some present in multiple copies, four of which are synthesised in the mitochondrion. This massive complex spans the inner mitochondrial membrane and comprises two major parts: F_0, which consists of hydrophobic subunits embedded in the inner membrane and which acts as an H^+ pore or channel; and F_1, which is hydrophilic and extends into the matrix on a 'stalk'. F_1 contains the active site of the ATP synthase and is a reversible ATPase. When connected to F_0, F_1 can either hydrolyse ATP and drive H^+ translocation into the intermembrane space, or, when $\Delta\mu_H{}^+$ drives H^+ back into the matrix through F_0, it can synthesise ATP from bound ADP and P_i. The stalk contains a protein known as the oligomycin-sensitivity-conferring-protein (OSCP) because it binds the antibiotic oligomycin which then prevents H^+ translocation through F_0 and inhibits ATP synthesis. Therefore, adding oligomycin to mitochondria oxidising a substrate in the presence of ADP restricts O_2 uptake (Figure 2.26).

The reaction mechanism of the ATP synthase remains controversial but the most favoured hypothesis is a

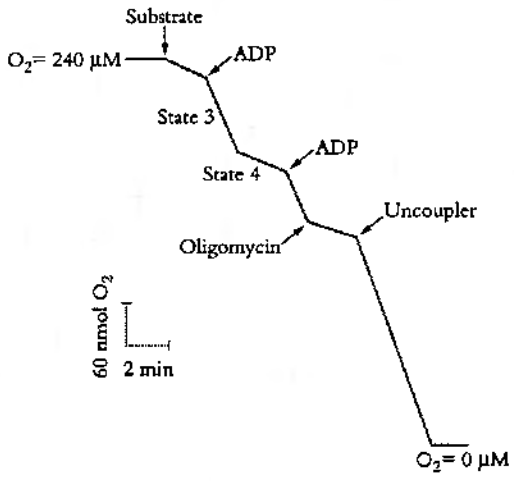

Figure 2.26 Stylised O_2 electrode recording of respiring plant mitochondria illustrating respiratory control. Oxygen consumption is measured as a function of time. The isolated mitochondria are depleted of substrates and are therefore dependent on added substrate. Addition of ADP (inorganic phosphate is in the reaction medium) allows oxidative phosphorylation to proceed, dissipating some of the protonmotive force and thereby stimulating electron transport; the enhanced rate of O_2 uptake is called State 3. When all added ADP is phosphorylated, electron transport slows to what is known as State 4 ('resting'state). Addition of more ADP stimulates O_2 uptake further, but addition of oligomycin, which blocks the ATP synthetase, lowers O_2 uptake to the State 4 rate. Addition of an uncoupler (protonophore) fully dissipates the protonmotive force and stimulates O_2 uptake; no ATP synthesis occurs in the presence of the uncoupler. When the O_2 concentration falls to zero, respiration ceases
(Original drawing courtesy David Day)

CASE STUDY 2.1 Knobs and ATP synthase

R.N. (Bob) Robertson

During the mid-1950s Marjorie Wilkins and I, both of CSIRO Food Preservation and Transport, were collaborating with John Farrant, CSIRO Industrial Chemistry. Using his electron microscope, we had seen what we then called 'knobs' protruding from the inner surfaces of plant mitochondria (Farrant *et al.* 1956).

Happily, the molecular structure of such bodies is now so well understood, thanks to the experiments of many workers around the world, that we have a good understanding of their function at a molecular level. As a retired plant physiologist, I have become specially interested in the membrane-bound F_0F_1ATPase of *E. coli*, also an ATP synthase. Here my thanks are due to the Frank Gibson (1991) and Graham Cox Group in John Curtain school at ANU, whose work led to my understanding the hypothesis of its structure and function.

The 'knobs' attached to a membrane-bound portion (Figure 1) are thought to be analogous to motors, with internal subunits that rotate at about 200 times per second relative to adjacent subunits, and with the stalk complex acting as a kind of 'stator'. According to this rotational model, protons are pumped across the membrane. Proton pumping in one direction results in formation of ATP from ADP and phosphate; in the other direction, ATP is hydrolysed to ADP, liberating H^+ ions, to which the movement of other ions is linked. Thanks to the techniques of molecular biology and to many workers, much of the structure is now understood. The 'knobs' in chloroplast membranes are similar in structure to those in mitochondria, but point the opposite way.

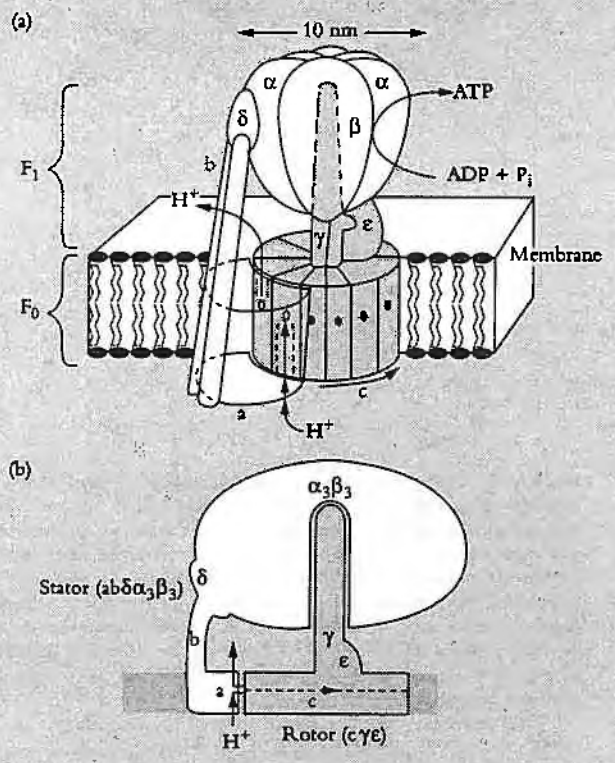

Figure 1 **Nature's tiniest rotary motor shown here as a highly diagrammatic version of an ATP synthase complex — a device for generating ATP from free energy stored as a transmembrane protonmotive force (a gradient in electrochemical potential of protons, consisting of a pH gradient and a gradient in electric potential). The ATP synthase complex of chloroplasts was referred to earlier as a 'coupling factor' (Figure 1.11). (a) In mitochondria, an asymmetric portion F_0 spans the inner membrane and provides a conduit for proton movement across this inner membrane (from intermembrane space to matrix), movement that imparts a torque between two adjacent subunits 'a' and 'c'. Torque so generated is transmitted to F_1 via the shaft 'γ' plus the 'ε' subunit. (b) 'a', 'b' and 'δ' subunits are linked to the F_1 hexamer ($\alpha_3\beta_3$) and constitute the 'stator' of this rotary motor. The 'rotor' itself is represented here as a shaded portion of the overall complex, and comprises 'c', 'γ' and 'ε' subunits. The 'γ' subunit behaves as a rotating shaft that mediates an exchange of energy derived from proton flow through F_0 for ATP synthesis via the cooperative activity of three catalytic sites within F_1 (three ATPs are generated for every 12 protons that pass through this rotary motor).**

In a widely acclaimed technical achievement, Hiroyuki Noji and colleagues at Yokohama (Noji *et al.* 1997) attached a fluorescent actin filament to the tip of a γ subunit and recorded continuous rotation during synthesis of ATP, thus confirming a rotary motion that had been predicted on biophysical grounds. Unrestrained by a long actin filament, rotation rate *in vivo* would peak around 150 revs per second.

Significantly, when provided with a source of ATP, this selfsame device (an ATP synthase complex) can draw energy from ATP hydrolysis to pump protons against a gradient. Now working as an ATPase, these rotary motors sustain energy-dependent processes including nutrient ion uptake and salt exclusion by plant roots

(Redrawn from Elston *et al.* 1998)

'conformational' model. According to this model, F_1 has three nucleotide-binding sites which can exist in three configurations: one with loosely bound nucleotides, one with tightly bound nucleotides and the third in a nucleotide-free state. H^+ movement through F_0 results in rotation of F_1 causing a conformational change during which the site with loosely bound ADP and P_i is converted to one which binds them tightly in a hydrophobic pocket in which ATP synthesis occurs. Further H^+ movement then causes another rotation of F_1 and the ATP binding site is exposed and releases the nucleotide. In the meantime, the other nucleotide-binding sites are undergoing similar changes, with ADP and P_i being bound and converted to ATP. Thus H^+ translocation drives the three sites through three different configurations and the main expenditure of energy is in the induction of a conformational change that releases tightly bound ATP, rather than in ATP synthesis itself.

(b) Respiratory control

Electron transport through the respiratory chain, and therefore rate of O_2 uptake, is controlled by availability of ADP and P_i, a phenomenon described as 'respiratory control'. In the absence of ADP or P_i, the proton pore of ATP synthase is blocked and a $\Delta\mu_{H^+}$ builds up to a point where it restricts fur-

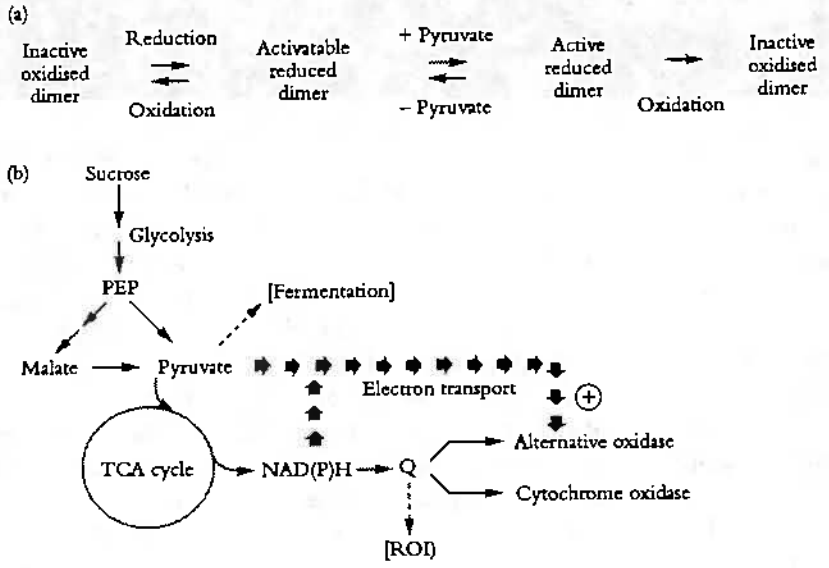

Figure 2.27 Regulation of alternative oxidase. (a) The alternative oxidase exists as a dimer linked together by disulphide bonds. Reduction of these bonds is required to allow activation of the oxidase; this activation occurs by a direct interaction between pyruvate and the oxidase. Oxidation inactivates the oxidase even when pyruvate is present. (b) Putative feed-forward regulation of the alternative oxidase to prevent fermentation from accumulated pyruvate and formation of reactive oxygen intermediates (ROI) from over-reduced ubiquinone (Q). *In vivo*, reduction of the oxidase is apparently achieved via NAD(P)H which will accumulate when carbon flux through the TCA cycle is high and/or the cytochrome chain is inhibited. Small solid arrows indicate activation pathways; dashed arrows indicate potentially deleterious side reactions
(Original drawing courtesy David Day)

ther H^+ translocation across the inner membrane. Since electron transport is functionally linked to H^+ translocation, this elevated $\Delta\mu_H{}^+$ will also restrict O_2 uptake. That outcome is easily seen with isolated mitochondria (Figure 2.26) where O_2 uptake is stimulated by adding ADP ('State 3' respiration). When all of the added ADP has been consumed, O_2 uptake decreases again ('State 4'). In steady state, the rate of electron flow is determined by the rate of flow of H^+ back across the membrane: when ADP and P_i are available the backflow is rapid and occurs via ATP synthase; in the absence of these compounds, backflow is no more than a slow leak. The ratio of State 3 to State 4 (the respiratory control ratio) is thus an indication of coupling between ADP phosphorylation and electron transport. Larger values represent tighter coupling. The proton leak can be dramatically stimulated by some compounds which act as protonophores or proton channels; these compounds collapse the $\Delta\mu_H{}^+$ and increase O_2 uptake up to the State 3 rate (Figure 2.26). However, no ATP is formed and these compounds are called uncouplers because they uncouple the linked processes of electron transport and phosphorylation.

2.4.7 An alternative oxidase

In both plants and animals, cytochrome oxidase is sensitive to a number of inhibitors, the best known of which are carbon monoxide and cyanide. Plants, however, show resistance to both carbon monoxide and cyanide because they are equipped with an alternative oxidase. This enzyme does not translocate H^+ and therefore is not linked to ATP formation. The enzyme is a quinol oxidase and appears to consist of one to three polypeptides of about 25–35 kDa, depending on the plant species. The proteins are encoded in nuclear genes which show tissue-specific expression. Cyanide-insensitive O_2 uptake is inhibited by hydroxamic acids (SHAM — salicyl

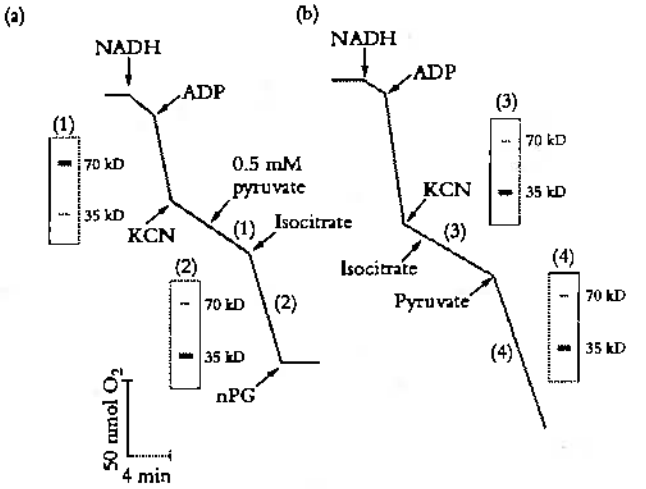

Figure 2.28 Experimental evidence for schemes in Figure 2.27. (a) and (b) represent oxygen electrode recordings obtained with a suspension of mitochondria isolated from tobacco leaves. NADH is added as the electron donor, and ADP ensures that electron transport is not restricted by the rate of oxidative phosphorylation. Addition of KCN inhibits cytochrome oxidase and thus allows alternative oxidase activity to be measured. At times indicated by (1)–(4), samples of mitochondria were taken from the reaction vessel, their proteins separated by SDS-PAGE in the absence of reductant, and alternative oxidase protein (AOX) bands visualised by immunoblotting (shown schematically as inserts).

At (1), pyruvate has been added to the mitochondria but the rate of cyanide-sensitive respiration remains low because AOX protein is largely oxidised (the covalently linked dimer is evident at 70 kD in the blot); however, when isocitrate is added at (2) to generate NADPH in the mitochondrial matrix, AOX becomes reduced (major band at 35 kD is seen in the blot) and cyanide-insensitive O_2 uptake becomes rapid as AOX is activated. At (3), isocitrate has been added and AOX is reduced, but respiration remains slow because pyruvate is not present to activate the enzyme fully. At (4), the redox status of AOX does not change, but AOX activity increases dramatically upon pyruvate addition. Thus both a *reductant* such as NADPH and an *activator* such as pyruvate must be present before the alternative oxidase is fully engaged. In this case NADPH was generated from isocitrate via NADP-linked isocitrate dehydrogenase in the mitochondrial matrix
(Based on Vanlerberghe *et al.* 1995)

hydroxamic acid — is the most commonly used) and n-propylgallate.

Activity of the alternative oxidase is regulated by a complicated feed-forward mechanism (Figure 2.27, with experi-

mental evidence in Figure 2.28). The oxidase exists in mitochondria as a dimer which can be inactivated by covalent linkage via disulphide bonds. Activation of the enzyme involves reduction of that bond, probably via matrix NADPH in a thioredoxin-mediated reaction. The reduced (but not the oxidised) enzyme is stimulated allosterically by pyruvate and some other 2-oxo acids (such as glyoxylate), which interact directly with the oxidase.

This activation by pyruvate was discovered almost by accident during collaborative research involving Harvey Millar and David Day (Australian National University) and Joe Wiskich (University of Adelaide). It began when Jim Siedow (Duke University, USA) emailed the ANU group to say that he could not repeat their published results showing that soybean root mitochondria have alternative oxidase activity. As became apparent, this difference was due to substrate. Harvey Millar (a fourth year honours student at the time) had been using a mixture of malate plus pyruvate as TCA cycle substrates for his isolated mitochondria, whereas Jim Siedow was using succinate. Harvey and David had gone to Adelaide to use the so-called 'Q' electrode of Joe Wiskich to investigate apparent differences between substrates in more detail. However, they could not repeat their results from Canberra. Much to their consternation, soybean root mitochondria in Adelaide were completely sensitive to cyanide. However, the Wiskich group routinely used a mixture of malate plus glutamate to drive the TCA cycle, and when pyruvate was added to the reaction vessel, mitochondrial preparations showed a dramatic stimulation of respiration despite the presence of cyanide. Significantly, the level of ubiquinol remained unchanged, implying that this effect was not simply due to oxidation of added pyruvate. A few frantic weeks of experimentation followed, resulting in a publication by Millar *et al.* (1993) on organic acid activation of the alternative oxidase of plant mitochondria, and illustrating the value of global communication between research groups.

Ubiquinol (Figure 2.23) is substrate for the alternative oxidase whose activity is also governed partly by the degree of reduction of the quinone pool. Where pyruvate is absent, the ratio of $Q_{reduced}/Q_{total}$ (QH_2/Q ratio) must be very high to activate the oxidase; when pyruvate is present, the alternative oxidase becomes active at a much lower QH_2/Q ratio (Figure 2.29) and can compete with the cytochrome chain for electrons, and efficiency of ATP generation diminishes. In Figure 2.29, ubiquinone reduction is presented as the ratio of fully reduced ubiquinol to total ubiquinone (oxidised or reduced). Kinetics of the cytochrome pathway are effectively linear with respect to ubiquinone reduction. Kinetics of the alternative pathway are sigmoidal with significant activity only apparent once the ubiquinone pool is half reduced. When pyruvate is present, alternative pathway kinetics shift to the left, allowing greater electron flux at lower ubiquinone pool reduction levels. Under those circumstances, the alternative pathway will compete with the cytochrome pathway for reduced ubiquinone. Saturation

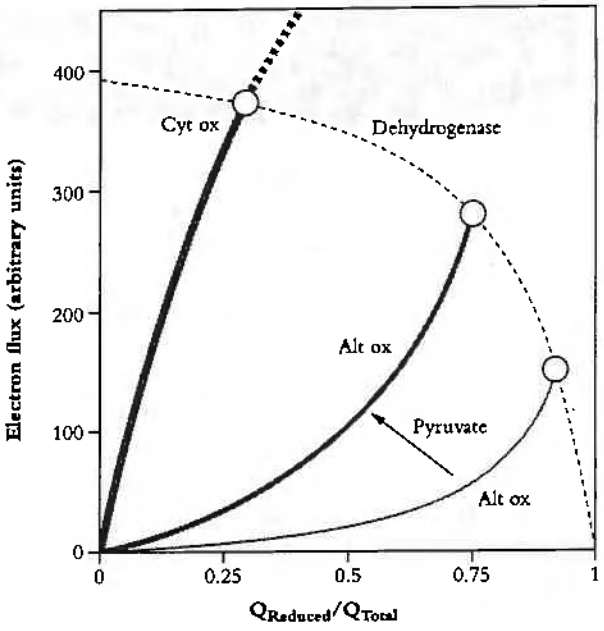

Figure 2.29 **Electron flux via either cytochrome oxidase (Cyt Ox) or the alternative oxidase (Alt Ox) varies according to the oxidation/reduction status of the quinone pool (Q). At low levels of reduced Q (i.e. a QH_2/Q ratio of 0.25 or thereabouts) electron flow via Cyt Ox is near capacity, whereas Alt ox contributes little to the overall flux of electrons to molecular oxygen, and thus production of H_2O. The Alt ox pathway becomes progressively engaged at higher values of the QH_2/Q ratio, and the extent of that engagement is greatly enhanced by pyruvate due to direct activation of the Alt ox pathway** (Original drawing courtesy Harvey Millar; derived from data in Hoefnagel *et al.* 1995 and fitted to the Q pool model of Van den Bergen *et al.* 1994).

of electron flux via either pathway is not observed in plant mitochondria as the mitochondrial dehydrogenases that provide the driving force for ubiquinone reduction usually become limiting long before either oxidase capacity is saturated. Consequently, the rate of electron flux at the steady-state level of ubiquinone reduction (ordinate in Figure 2.29) will be at the point of intersection between dehydrogenase and oxidase pathway kinetics (open circles in Figure 2.29).

These different controlling factors seem to form part of a regulatory mechanism that ensures that the alternative oxidase is 'turned on' when carbon flux through the cell is high or when the cytochrome chain is inhibited (e.g. by high cytosolic ATP/ADP). Under these conditions, pyruvate and reduced pyridine nucleotide levels will be relatively high, ensuring reduction and activation of the oxidase. This mechanism may point to a protective role for the alternative oxidase, preventing accumulation of pyruvate (which may lead to fermentation) and over-reduction of respiratory chain components (which may cause generation of damaging reactive oxygen species such as superoxide ions). Exposure of plants to low temperatures may cause disruption of the cytochrome path (probably via lipid phase changes) and the alternative oxidase may play a role here, since cold treatment stimulates its synthesis. Alternative oxidase synthesis is also induced by other conditions of stress including pathogen attack and ethylene-triggered processes such as fruit ripening, as well as by cytochrome chain inhibitors, all suggesting a protective role.

FEATURE ESSAY 2.2 Thermogenesis

Joe Wiskich

Respiration is a combustive process and about 75% of its free energy is used to phosphorylate ADP to ATP. Cells tend to maintain very high ATP/ADP ratios and this places a limitation on the rate of respiration via allosteric inhibition of glycolysis and via respiratory control applied to the mitochondrial electron transfer chain.

Heat generation is a useful phenomenon in plants, and is used to melt snow or volatise aromatic compounds to attract insects. To generate heat it is necessary to have inefficient ATP-utilising processes and a rapid rate of respiration. This can be achieved by 'futile cycles' whereby ATP and a kinase phosphorylate a metabolite and a phosphatase re-generates it. The net result of this process is the hydrolysis of ATP to ADP and P_i, producing both heat and ADP which allows for rapid respiration. Bumblebees use such a cycle in cold weather to warm up their muscles before 'take off'. If we are cold, we tend to shiver which produces the same effect.

Another way of achieving heat production is not to make ATP in the first place. Hibernating animals have brown adipose tissue whose mitochondria contain 'thermogenin' (a proton-translocating protein) in their inner membranes. When this protein is functional it prevents the establishment of a protonmotive force across the inner mitochondrial membrane and the free energy of respiration is liberated as heat. We are born with some of this brown adipose tissue but lose it early in life.

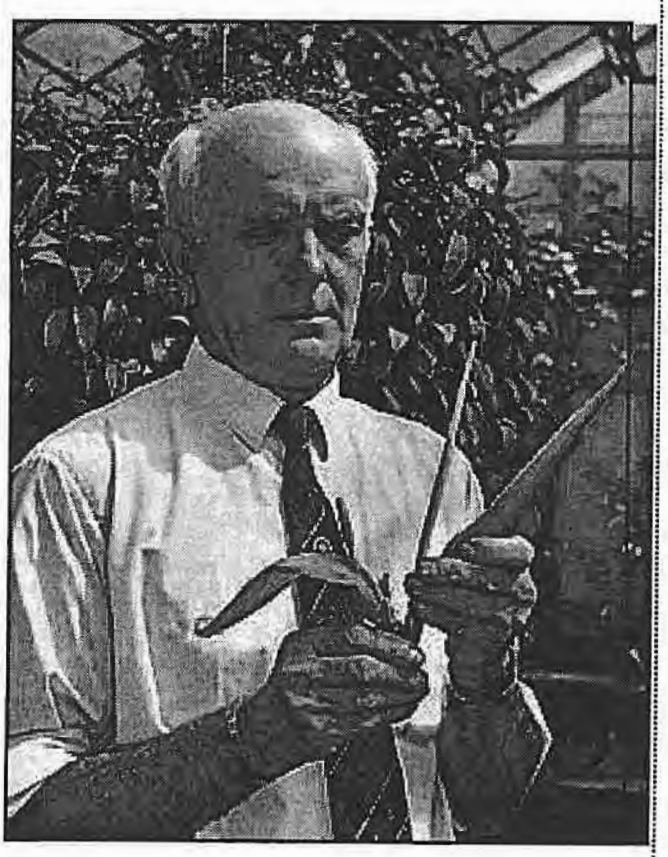

Figure 1 Joe Wiskich (Botany Dept, University of Adelaide) examines spadices of Arum maculatum (left) and Dracunculus vulgare (right) collected from the Adelaide Botanic Garden. Both species heat their spadices via 'futile cycles' of respiratory metabolism to volatilise aromatic compounds and attract pollinating insects

Plants also produce heat, as was observed by Lamarck in 1788. The family Araceae has more than 100 genera and about 3000 species. In many aroids the fertile flowers are clustered around a central spadix which is full of respiratory fuel. This can be mainly carbohydrate (as in *Arum*) or a mixture of carbohydrate and fat (as in *Philodendron*). In these plants the spadix can increase its respiratory rate 100-fold and raise its temperature above 40°C. The actual increase can be 20–30°C depending on the ambient temperature. For example, the inflorescence of the skunk cabbage (*Symplocarpus foetidus*) melts the snow as it grows up through it. Generally, the aroids generate heat to volatise aromatic compounds which attract insects to facilitate cross-pollination. The process plants use for this purpose differs from the 'thermogenin' protein of brown adipose tissue but achieves the same result. The mitochondria of thermogenic plants contain an 'alternative oxidase' which branches from the mitochondrial electron transfer chain at ubiquinone. This is the alternative path and differs from the cytochrome path in that it does not conserve energy (to produce ATP) and is insensitive to cyanide and other inhibitors of cytochrome oxidase.

The aroid spadices with their heat production, rapid respiration rates and complete insensitivity to cyanide were considered to be the 'type-specimens' for cyanide-insensitive respiration. However, other plants showed only partial sensitivity to cyanide and these were regarded as 'cyanide resistant'. Even those tissues completely sensitive to cyanide could be 'induced' to become cyanide resistant, for example fresh potato tuber slices are sensitive but become resistant on ageing. Thus, the alternative path is a feature potentially available to all higher plant mitochondria and at some stage during the development of any tissue is likely to become important. Inducing the alternative path really means inducing or activating the terminal 'alternative oxidase'.

In 1987 Pierre Rustin questioned the nature of the alternative oxidase; was it a ubiquinol oxidase? Were we measuring quinol auto-oxidation? Could it be a lipoxygenase or was it a 'free radical' mechanism? Some of the problems we had at that stage were: first, the reactivity of the alternative oxidase to some substrates was different in mitochondria from thermogenic compared to non-thermogenic tissues; second, the activity could only be solubilised from

thermogenic mitochondria; third, attempts to purify it were only partially successful; and, finally, some results were being interpreted in terms of different ubiquinone pools existing within the membranes so that the NADH from some matrix enzymes (NAD-malic enzyme) had better access to the alternative oxidase than others (NAD-malic dehydrogenase). Since then a number of significant events have occurred.

My laboratory was investigating photorespiratory metabolism in pea leaf mitochondria and we had difficulty interpreting some of our results. We could explain our data if we assumed either a mixed population of mitochondria or a differential access of NADH generated by the oxidation of glycine to the electron transport chain compared to the NADH generated by malate oxidation. We eliminated the first possibility with some immunogold-labelling studies, and it was to test the second that Tony Moore (University of Sussex, UK) come to my laboratory with a so-called Q electrode. This measured the redox state of the inner-membrane pool of ubiquinone-10, using a more water soluble quinone analogue as a mediator.

David Day (Australian National University) also visited at this time and brought with him some soybean mitochondria; these have a reasonable degree of alternative path activity. So for the first time we were able to measure simultaneously the rate of alternative oxidase activity and the redox state of its substrate. The initial results were quite clear — the alternative oxidase showed little activity until the ubiquinone pool was about 50% reduced and increased quite markedly above that. The cytochrome path became active as soon as some ubiquinone was reduced and reached apparent saturation at 20–30% reduction. These results appeared to validate, in general — but not precise — terms, the Bahr and Bonner hypothesis that the cytochrome path had to be saturated before any flux through the alternative path could be observed.

However, we still had problems. In soybean mitochondria succinate and NADH reduced the ubiquinone pool to the same extent, yet the alternative path oxidised succinate much more rapidly. Reduced quinone analogues were also poor substrates. It was Harvey Millar in David Day's laboratory who noticed that malate oxidation via the alternative oxidase was much faster if pyruvate, rather than glutamate, was used to remove the oxaloacetate. It was soon established that pyruvate and other 2 oxo-acids such as glyoxylate, oxaloacetate and 2-oxoglutarate activated the alternative oxidase. In the presence of pyruvate, soybean mitochondria oxidised NADH and quinol analogues via the alternative oxidase. So the real problem was the availability of pyruvate — substrates which could produce pyruvate and activate the alternative oxidase were more readily oxidised than those that didn't. This solution to one problem highlighted another. When we repeated our analyses on the relationship between the redox state of the ubiquinone pool and rates of O_2 uptake it became obvious that the alternative oxidase was very active at a relatively low level of ubiquinone reduction. This meant that the alternative path was now competing with the cytochrome path and electron flow could 'switch' from one pathway to the other. A wealth of data on estimating the contribution of the alternative oxidase to tissue respiration (so-called 'engagement' or 'rho' determinations) now had to be treated with great caution. This is because the technique used inhibitors and assumed electron flow could not switch from the alternative to the cytochrome path. Further, any inhibition of the electron transfer chain in tissues could lead to an increase in the concentration of pyruvate.

We believe that pyruvate activation eliminates the problems associated with preferential oxidation of substrates via the alternative oxidase. There are still differences in kinetics of the alternative oxidase with respect to the redox state of ubiquinone among mitochondria from different tissues. However, I feel that these should be considered in terms of the balance between input and output from the ubiquinone pool. When Peter Rich (Glynn Research Institute, Bodmin, UK) visited my laboratory he brought some very potent alternative oxidase inhibitors with him. Using these we estimated that *Arum* and soybean mitochondria contain 720 and 58 pmol alternative oxidase mg^{-1} mitochondrial protein. Clearly a mitochondrion with a high amount of the enzyme will maintain faster rates of O_2 uptake at lower levels of reduced ubiquinone.

Meanwhile, advances were being made in North America. Tom Elthon, in Lee McIntosh's laboratory (Michigan State University,) had produced an antibody to alternative oxidase which cross-reacted with proteins from a wide range of plants. The alternative oxidase, when reduced, was detectable on electrophoresis gels in the range of 32 to 37 kDa. There appears to be three separate protein forms which exist in varying combinations in different tissues. Subsequently, David Rhoads and Lee McIntosh isolated the genes from both thermogenic and non-thermogenic tissues. Thus, the alternative oxidase finally reached the status of being a real protein, a nuclear-encoded enzyme. From Jim Siedow's laboratory (Duke University, North Carolina), Ann Umbach reported that the enzyme could exist as an inactive oxidised dimer bringing attention to regulation by its redox state, involving sulphydryl–disulphide interactions. This has physiological implications. David Day and I received an Australian government DITAC Collaborative Research Award to visit Lee McIntosh, who had produced transgenic tobacco plants over- and under-expressed in alternative oxidase protein. Although mitochondria isolated from the leaves of over-expressed plants contained more alternative oxidase protein than did wild type, their activity was the same. However, full activity was elicited by reducing the enzyme, which could be achieved by adding citrate. We suggest that NADP-isocitrate dehydrogenase produces

NADPH which reduces the enzyme, most probably via a thioredoxin-type process.

We now have a feed-forward system to activate the alternative oxidase. It depends on an increase in the supply of mitochondrial substrate which can both reduce the alternative oxidase and activate it. In normal metabolism pyruvate appears to be important and this is usually considered to arise from pyruvate kinase but it must be remembered that plant mitochondria contain NAD-malic enzyme and can produce their own pyruvate from any Kreb's cycle intermediate. During photorespiration in C_3 leaves the supply of glycine to mitochondria is very rapid. Assuming the photorespiratory rate to be about 25% of net CO_2 fixation the generation of reducing power within the mitochondria would be two to three times that of dark respiration. The fate of this reducing power is problematical—some finding its way to the peroxisomes for hydroxypyruvate reduction and some being oxidised by the electron transport chain. If there are problems in eliminating the reducing power, glyoxylate concentrations would rise and activate the alternative oxidase.

The role of the alternative path in thermogenic aroids has been mentioned. In other plants, its gene expression is induced by cold, so it may have a general role in warming plant tissues. However, it is present in all plants and can be induced by heat, drought, nutrient deficiency, insect and fungal attack, treatment with poisons — in fact any stressful situation — so it must have a more general role as well.

I recall some scientists considering the alternative path to be 'wasteful' respiration and who grew plants in the presence of alternative oxidase inhibitors. Presumably, they expected to get bigger and better plants; another great idea ruined by an ugly fact — the plants died. It seems to me that the alternative oxidase is present, perhaps to generate some heat (certainly among some plant scientists if not plants), but also to maintain the redox state of the cell at some maximum level of reduction. What causes the tissues to become over-reduced is secondary and of little consequence. Once the tissue reaches a critical value of reduction the alternative oxidase swings into action — if there is insufficient enzyme the gene is signalled to produce more. Over-reduction can lead to the production of deleterious superoxides. The alternative path allows the respiratory pathways to produce intermediates without being sulyceted to severe oderylate control.

Further reading

Day, D.A., Whelan, J., Millar, A.H., Soedow, J.N. and Wiskich, J.T. (1995). 'Regulation of the alternative oxidase in plants and fungi', *Australian Journal of Plant Physiology*, **22**, 497–509.

McIntosh, L. (1994). 'Molecular biology of the alternative oxidase', *Plant Physiology*, **105**, 781–786.

Meeuse, B.J.D. (1975). 'Thermogenic respiration in aroids', *Annual Review of Plant Physiology*, **26**, 117–126.

2.4.8 Interactions between mitochondria and chloroplasts

One dominant interaction between mitochondria and chloroplasts involves metabolite exchange as part of the photorespiratory carbon/nitrogen cycle, but more subtle interactions also occur. For example, respiratory ATP production in the light is required to maintain maximum photosynthetic activity (Krömer 1995). Experimentally, if oligomycin is used to disrupt oxidative phosphorylation of mitochondria in leaf cells, photosynthesis is inhibited even though oligomycin is specific to mitochondrial ATP synthase at the concentrations applied (Krömer 1995). Clearly, a link must exist between mitochondrial ATP synthesis and photosynthesis via the energy demands of sucrose synthesis (because of sucrose phosphate synthase). A decline in supply of ATP decreases the rate of sucrose synthesis and this affects the rate of photosynthetic metabolism in chloroplasts. Using a different approach to this same issue, Shyam *et al.* (1993) inhibited production of mitochondrial ATP with azide and/or the uncoupler FCCP and exacerbated photoinihibition in pea leaves. Their results confirm interplay between chloroplasts and mitochondria, and suggest a protective role for mitochondria, perhaps by provision of energy for chloroplast repair.

Leaf respiration rates are commouly measured in darkness, as either CO_2 release or O_2 consumption. Such measurements are complicated in light by reverse gas exchange from photosynthesis. None the less, indirect measurements involving the compensation point suggest that CO_2 release is inhibited in light relative to that in dark (Brooks and Farquhar 1985). Such inhibition of CO_2 release in light involves a decrease in carbon flow through the TCA cycle and does not seem to involve photorespiration. In contrast, respiratory O_2 consumption (excluding that associated with glycine decarboxylation) is stimulated in light compared to that in darkness. Put another way, while TCA cycle activity is decreased in light, electron transport may increase.

This apparent paradox can be explained. During active photosynthesis (non-photoinhibitory conditions), mitochondria in a leaf cell are able to oxidise surplus redox equivalents arising from photosynthetic electron transport. Those redox equivalents are then exported from the chloroplast via the malate–OAA shuttle or the DHAP–PGA shuttle (Krömer and Heldt 1991). Under these conditions, mitochondria would oxidise cytosolic NAD(P)H rather than that generated by the TCA cycle.

Coincidentally, the importance of exporting photosynthetic reducing equivalents to the mitochondria appears to increase during cold hardening (Hurry *et al.* 1995) and may

assist in preventing photoinhibition. It is also possible that the export of α-ketoglutarate from the mitochondrion for nitrate reduction (see above) may lead to a decrease in CO_2 release from the TCA cycle; nitrate reduction is greater in the light because of the need for photosynthetic reduction of nitrite, the next step in this reaction sequence.

2.4.9 Energetics of respiration

Efficiency

Respiration represents a substantial loss of carbon from a plant, and under adverse conditions can be as high as two-thirds of the carbon fixed daily in photosynthesis. Both the rate and the efficiency of respiration will therefore affect plant growth significantly. The overall process of respiration results in the release of a substantial amount of energy which may be harnessed for metabolic work. In theory, the energy released from the complete oxidation of one molecule of glucose to CO_2 and H_2O in the respiratory reactions leads to the synthesis of a net equivalent of 36 molecules of ATP. However, in plants, because there are alternative routes for respiration, this yield can be greatly reduced.

Mechanisms for regulating respiration rates in whole plants remain unclear. Convention has it that the rate of respiration is matched to the energy demands of the cell through feedback regulation of glycolysis and electron transport by cytosolic ATP/ADP. However, since plants have non-phosphorylating bypasses in their respiratory chain that are insensitive to ATP levels, and since PEP carboxylase and PFP might be involved in sucrose degradation, the situation *in vivo* is not so simple. For example, the rotenone-insensitive bypass of complex I requires high concentrations of NADH in the matrix before it can operate and seems to be active only when substrate is plentiful and electron flow through complex I is restricted by lack of ADP. Alternative oxidase activity also depends on carbon and ADP availability. In other words, non-phosphorylating pathways act as carbon or reductant 'overflows' of the main respiratory pathway and will only be active *in vivo* when sugar levels are high and the glycolytic flux rapid, or when the cytochrome chain is inhibited during stress. In glycolysis, the interaction between environmental signals and key regulatory enzymes, as well as the role of PFP and its activator fructose-2,6-P_2, will be important.

Allocation of respiratory energy to process physiology

One way of viewing respiratory cost for plant growth and survival is by subdividing measured respiration into three components associated with (1) nutrient acquisition, (2) growth and (3) maintenance. Such conceptual distinctions are somewhat arbitrary, and these categories of process physiology must not be regarded as three discrete sets of biochemical events. Such energy-dependent processes are all interconnected to some extent because ATP represents a universal energy currency for all three, while a common pool of substrates is drawn upon in sustaining production of that ATP (Amthor 1989). Nevertheless, cells do vary in their respiratory efficiency, while genotype × environment interactions are also evident in both generation and utilisation of products from oxidative metabolism. Such variation has implications for growth and resource use efficiency (Section 6.5).

Further reading

ap Rees, T. (1980). 'Assessment of the contributions of metabolic pathways to plant respiration', in *The Biochemistry of Plants*, Vol. 2, ed. D.D. Davies, 1–29, Academic Press: New York.

Copeland, L. and Turner, J.F. (1987). 'The regulation of glycolysis and the pentose phosphate pathway', in *The Biochemistry of Plants*, Vol. 11, ed. D.D. Davies, 107–28, Academic Press: San Diego.

Douce, R. and Joyard, J. (1990). 'Biochemistry and function of the plastid envelope', *Annual Review of Cell Biology*, **6**, 173–216.

Douce, R. and Neuburger, M. (1989). 'The uniqueness of plant mitochondria', *Annual Review of Plant Physiology and Plant Molecular Biology*, **40**, 371–414.

Douce, R. and Neuberger, M. (1992). 'Metabolite exchange between the mitochondria and the cytosol', in: *Plant Physiology, Biochemistry and Molecular Biology*, eds. D.T. Dennis and D.H. Turpin, 173–190, Longman Scientific and Technical, Harlow.

Dry, I.B., Bryce, J.H. and Wiskich, J.T. (1987). 'Regulation of mitochondrial metabolism', in *The Biochemistry of Plants*, Vol. 11, ed. D.D. Davies, 213–352, Academic Press: London.

Flügge, U.I. and Heldt, H.W. (1991). 'Metabolite translocators of the chloroplast envelope', *Annual Review of Plant Physiology and Plant Molecular Biology*, **42**, 129–144.

Lambers, J.T. and van der Plas, L.H.W. (eds) (1992) *Biochemical and Physiological Aspects of Plant Respiration* SPB Academic Publishing: The Hague.

Martinoia, E. and Rentsch, D. (1994). 'Malate compartmentation-responses to a complex metabolism', *Annual Review of Plant Physiology and Plant Molecular Biology*, **45**, 447–467.

Siedow, J.N. and Umbach, A.L. (1995). 'Plant mitochondrial electron transfer and molecular biology', *The Plant Cell*, **7**, 821–831.

Stitt, M. (1990). 'Fructose-2,6-bisphosphate as a regulatory metabolite in plants', *Annual Review of Plant Physiology and Plant Molecular Biology*, **41**, 153–185.

Stitt, M. and Steup, M. (1985). 'Starch and suctose degradation', in *Encyclopedia of Plant Physiology* (New Series), Vol. 18, eds R. Douce and D.A. Day 347–390, Springer-Verlag: Heidelberg.

Wink, M. (1993). 'The plant vacuole: a multifunctional compartment', *Journal of Experimental Botany*, **44**, 231–246.

3 *Gaining water and nutrients (root function)*

A radicle may be compared with a burrowing mole, which wishes to penetrate perpendicularly into the ground. By continually moving its head from side to side, or circumnutating, he will feel any stone or other obstacle, as well as any difference in the hardness of the soil, and he will turn from that side; if the earth is damper on one than the other side he will turn thitherward as a better hunting-ground. Nevertheless, after each interruption, guided by the sense of gravity, he will be able to recover his downward course and burrow to a greater depth.

(Charles Darwin, The Power of Movement in Plants, *1881)*

Seedlings of *Eucalyptus globulus* which have formed an ectomycorrhizal association with the fungus, *Hebeloma*, whose white mycelium can be seen ramifying through the soil and forming basidiomes (toadstools) above the soil. (see Colour Plate xx)

Chapter outline